Growth Cones, Dying Axons, and Developmental Fluctuations in the Fiber Population of the Cat's Optic Nerve

ROBERT W. WILLIAMS, MICHAEL J. BASTIANI, BARRY LIA, AND
LEO M. CHALUPA
Department of Psychology and Physiology Graduate Group, University of California,
Davis, California 95616 (R.W.W., B.L., L.M.C.), and Department of Biological Sciences,
Stanford University, Stanford, California 94305 (M.J.B.)

ABSTRACT

We have studied the rise and fall in the number of axons in the optic nerve of fetal and neonatal cats in relation to changes in the ultrastructure of fibers, and in particular, to the characteristics and spatiotemporal distribution of growth cones and necrotic axons.

Axons of retinal ganglion cells start to grow through the optic nerve on the 19th day of embryonic development (E-19). As early as E-23 there are 8,000 fibers in the nerve close to the eye. Fibers are added to the nerve at a rate of approximately 50,000 per day from E-28 until E-39—the age at which the peak population of 600,000–700,000 axons is reached. Thereafter, the number decreases rapidly: About 400,000 axons are lost between E-39 and E-53. In contrast, from E-56 until the second week after birth the number of axons decreases at a slow rate. Even as late as postnatal day 12 (P-12) the nerve contains an excess of up to 100,000 fibers. The final number of fibers— 140,000–165,000—is reached by the sixth week after birth.

Growth cones of retinal ganglion cells are present in the optic nerve from E-19 until E-39. At E-19 and E-23 they have comparatively simple shapes but in older fetuses they are larger and their shapes are more elaborate. As early as E-28 many growth cones have lamellipodia that extend outward from the core region as far as 10 μm. These sheetlike processes are insinuated between bundles of axons and commonly contact 10 to 20 neighboring fibers in single transverse sections. At E-28 growth cones make up 2.0% of the fiber population; at E-33 they make up about 1.0%; from E-36 to E-39 they make up only 0.3% of the population. Virtually none are present in the midorbital part of the nerve on or after E-44. At all ages growth cones are more common at the periphery of the nerve than at its center. This central-to-peripheral gradient increases with age: at E-28 the density of growth cones is two times greater at the edge than at the center but by E-39 the density is four to five times greater.

Necrotic fibers are observed as early as E-28 in all parts of the nerve. Their axoplasm is dark and mottled and often contains dense vesiculated structures. From E-28 to E-39 an average of about 0.15% of all fibers are obviously necrotic, whereas during the most acute phase of fiber elimination—between E-44 and E-48—up to 0.4% are necrotic. Thereafter, their incidence is typically under 0.05%. Necrotic axons are scattered throughout the nerve. We estimate that the time required to clear away the debris of single axons is short—on the order of 1 hour—and on the basis of this estimate, we conclude that between 100,000 and 200,000 axons are lost even before the peak population of 700,000 is reached.

Taking into account the early loss of fibers, we estimate that a total of 800,000–900,000 retinal ganglion cell axons are produced in the fetal cat over a 20-day period from E-19 to E-39. Remarkably, only 20% survive to adulthood. The loss of fibers begins a few days before axons penetrate the thalamus (Shatz,'83), about 2 weeks before the onset of synaptogenesis in the dorsal lateral geniculate nucleus (Shatz and Kirkwood, '84), and more than 3 weeks before the segregation of retinal projections (Williams and Chalupa, '82,'83a; Shatz, '83; Chalupa and Williams, '84). The elimination of axons also persists long after the segregation of axon arbors from right and left eyes is complete, and as many as 100,000 axons are lost even after eye opening during a 1-month period when retinal arbors are still undergoing remarkable changes in shape and connectivity (Mason, '82a,b; Sur et al, '84).

A great excess of axons are produced and subsequently lost during the early development of the avian and mammalian optic nerve. Although there have been numerous quantitative studies of the nerve during development, we still know little about the relationship between this rise and fall in axon number and the corresponding changes in the nerve's ultrastructure (Rager and Rager, '76; Rager, '80; Ng and Stone, '82; Rakic and Riley, '83a; Perry et al., '83; Sefton and Lam, '84; Kirby and Wilson, '84; Provis et al., '85; Crespo et al., '85; Lia et al., '86). Our main aim has been to fill this gap: to provide a complete description of the maturation of the optic nerve—both qualitative and quantitative—and to answer the following specific questions.

•When are growth cones present in the nerve and what are their characteristics? The resolution of these questions, which are of broad relevance to issues of axon elongation, requires a detailed analysis of growth cone ultrastructure, number, and distribution within the nerve throughout development.

•When are axons eliminated from the nerve and what are the signs of axon elimination? Although it is clear that a large proportion of axons are lost spontaneously during normal development, almost nothing is known about the ultrastructure, distribution, or timing of axon elimination.

•What is the total number of axons produced during the formation of the optic nerve? It is generally assumed that the total production of axons equals the peak number of axons in the nerve, but this assumption is not valid if proliferative and degenerative phases of development overlap; that is, if there are both growth cones and necrotic axons in the nerve at the same time. By obtaining information on the duration of overlap of axon ingrowth and necrosis, it should be possible to determine to what extent the peak number underestimates the total production of fibers.

We have chosen to study the cat's optic nerve because so much is known about the genesis and maturation of this species' retina (Martin, 1891; Donovan, '66; Cragg, '75; Morrison, '77, '82; Rusoff and Dubin, '77; Vogel, '78; Greiner and Weidman, '80; Polley et al., '81; Kliot and Shatz, '82; Stone et al., '82; Rapaport and Stone, '82, '83; Lia et al., '83; Walsh et al., '83; Mastronarde et al., '84; Walsh and Polley, '85), and because the sequence of retinal innervation of the cat's dorsal lateral geniculate nucleus, pretectum, and superior colliculus has been well studied (Cragg, '75; Winfield et al., '80; Williams and Chalupa, '82, '83a; Mason, '82a,b; Shatz, '83; Sretavan and Shatz, '84; Chalupa and Williams, '85). This rich background provides an opportunity to correlate changes in the fiber population of the optic nerve with the development of the visual system.

MATERIALS AND METHODS
Animals and the determination of gestational age

This study is based on an analysis of 19 optic nerves taken from cats ranging in age from the 19th day of gestation (E-19) to the end of the third postnatal month. Litters of known gestational age were obtained by placing an estrous female together with a tomcat for 24 hours. Ovulation in cats occurs 24–30 hours after mating (Greulich, '34; Herron and Sis, '74) and the ova are viable for an additional 24 hours (Hoogeweg and Folkers, '70). Fertilization therefore occurs the day after mating—embryonic day 1 or E-1. In our colony most cats give birth within a day or two of E-65. However, viable offspring can be born as early as E-58 or as late as E-70 (Marin-Padilla, '71; Prescott, '73; Stein, '75).

Surgical and histological procedures

Pregnant females were anesthetized with 1.5% Halothane in oxygen or by an intravenous infusion of sodium pentobarbital. Incisions were made through the abdomen and uterus, and fetuses were removed one at a time and perfused immediately through the heart with 5–10 ml of saline followed by a fixative made up of 2% glutaraldehyde, 1% paraformaldehyde, 1% dimethyl sulfoxide, and 5 mM magnesium chloride in 0.05 M sodium phosphate buffer (pH of 7.4 ± 0.1) used at room temperature. In the youngest embryos (E-19 and E-23) with crown-to-rump lengths of 12–15 mm the saline rinse was omitted and the perfusion was begun immediately with fixative at a pressure of approximately 500–600 mm of water. The fixative was also injected behind the eye into the orbit. Postnatal animals were deeply anesthetized with an intraperitoneal injection of sodium pentobarbital and perfused transcardially as above.

Optic nerves were dissected in cold buffer. The dural sheath was removed gently, and the nerves were cut into short segments. Those pieces chosen for analysis were from the orbital portion of the nerve and were usually taken 1–3 mm from the eye. The eyes and nerves that were removed from the youngest animals, E-19 and E-23, were left intact. Following a wash in buffer, tissue was placed in a solution

of 2% osmium tetroxide for 1 hour, stained with 2% aqueous uranyl acetate, dehydrated, and embedded in Epon-Araldite. Semithin sections were cut at 1.0 μm for light microscopy and ultrathin sections were cut at about 0.08 μm for electron microscopy. Ultrathin sections were mounted on Formvar-coated slot-grids or on uncoated 400-mesh grids and stained with uranyl acetate and lead citrate. The 1-μm-thick sections were stained with a mixture of Azur II and methylene blue.

Sampling, measuring, and counting of fibers

Except at the earliest stage of development it was not practical to count all fibers in the optic nerve. Instead an estimate of the total number was made on the basis of the average density of axons in a representative set of micrographs. To obtain reliable and accurate estimates we employed without modification a procedure described in our previous studies (Williams et al., '83; Williams and Chalupa, '83b). Micrographs intended for counting were taken with Zeiss or Hitachi electron microscopes at instrumental magnifications ranging from 1,400 to 12,000. The sampled sites were distributed with as much uniformity as possible across the entire section of the nerve, and therefore, each region of the nerve was represented in proportion to its contribution to the total area of the tranverse section. Exposures were also taken without regard for the particular elements, be they axonal, glial, or vascular, that happened to dominate the field of view.

A variety of sampling strategies have been employed to estimate the number of axons in the optic nerve, including simple random sampling (Rhoades et al., '79), sampling along two or more diameters (Rakic and Riley, '83a), sampling each major fascicle (Easter et al., '81), and sampling systematically (Vaney and Hughes, '77). We chose to sample systematically using the square grid method (Cochran, '63, p. 229), both because this technique provides a simple and economical way to get a representative sample and because such systematic samples usually give estimates with less variance than do random samples of corresponding size (Cochran, '63, pp. 223–229). It is important to recognize that within wide limits, the accuracy of the method we employed depends far more on the number of sampled sites than upon the percentage of the area that is sampled (see Snedecor and Cochran, '67, p. 513). Therefore, no attempt was made to sample equal proportions of the nerves. In several sections obtained from the youngest embryos (E-19 and E-23) it was possible to make complete high-magnification (×8,000) montages and count all axons.

Calculation of fiber number. To estimate the number of axons in the optic nerve three values were determined: (1) the total area of the nerve in the particular ultrathin section that was photographed, (2) the area of nerve covered by the sample of micrographs, and (3) the number of axons within the area that was sampled. An estimate of the total population was then calculated by multiplying the number of axons that were counted by the ratio of the nerve area and the sampled area.

Accurate measurements of area were obtained using a calibration grid (0.214 μm²/grid unit, specified as accurate to within 0.05%, Ernest F. Fullam, Inc., U.S.A.). Areal magnification—the square of linear magnification—was then determined by counting the total number of grids covered by the calibration micrographs, and the square root of this value was used to calculate the *mean* linear magnification. This value was used to calculate the area of individual

micrographs and of low-power photomontages of the nerves.

The number of axons in each micrograph was determined by using Gundersen's rule ('77). His method is slightly more accurate than that usually employed to correct for the discrepancy between the *effective* sampling area and the *actual* micrograph area. This discrepancy, termed the "edge effect," arises when axons of which only small parts are within the margins of the micrograph are nevertheless counted. If uncorrected, the inclusion of these marginal fibers leads to an effective sample area greater than the actual micrograph area. The correction involved excluding from the count all axons that intersected the lower or left edges, or that intersected any corner other than the upper right corner. All counts were checked twice.

Accuracy of estimates. The accuracy of estimates of axon number depends upon two factors: (1) the sample size and its spatial resolution in relation to gradients of axon density, and (2) the accuracy of the count and of the measurements of area. The adequacy of the sample can be tested by breaking the pool of micrographs into subgroups and using these to calculate a number of "minority" estimates (Williams et al., '83). Four nerves were tested by using this procedure and the mean divergence of these estimates was less than 5%. We also determined the *reliability* of our sampling method by estimating the axon complement within two ultrathin sections cut from either side of a 1-mm-long segment of the nerve. The sections were photographed with different microscopes (Zeiss EM109 and Zeiss 10), and prints were made on different enlargers. Procedural details, however, were identical. Final estimates differed by less than 4% (Table 1).

TABLE 1. Size and Character of Axon Population of the Optic Nerve During Development

Age	No. of axons[*]	Area of nerve (μm²)	Axon density (100 μm²)	Necrotic fibers (%)	Growth cones (%)
E-19	88	2,300	3.8	0	[†]
E-23[‡]	8,000 ± 1,500	3,800	210	[§]	[†]
E-28	43,000 ± 3,000	13,000	330	0.23	2.0
E-33	292,000 ± 12,000	43,900	665	0.09	1.0
E-36	490,000 ± 28,000	76,500	645	0.10	0.3
E-39**	557,000 ± 28,000	74,400	749	0.21	0.3
E-39**	698,000 ± 20,000	95,700	729	0.26	0.2
E-44††	580,000 ± 13,000	93,000	623	0.41	<0.05
E-44††	457,000 ± 21,000	88,100	518	0.40	0
E-47	403,000 ± 31,000	124,000	325	0.15	0
E-48	328,000 ± 17,500	148,300	221	0.28	0
E-52	308,000 ± 30,000	179,500	172	[*]	0
E-53	225,000 ± 18,000	177,000	127	<0.05	0
E-56	230,000 ± 21,000	157,800	146	<0.05	0
E-61	267,000 ± 18,900	331,000	81	<0.05	0
P-2	293,000 ± 19,400	442,900	89	<0.05	0
P-12	250,000 ± 6,200	494,800	51	0.19	0
P-36	158,000 ± 9,500	1,200,000	13	0.22	0
P-84	162,000 ± 8,300	1,025,000	15	0.05	0

*To calculate standard error of the mean we first calculated the standard deviation of the number of axons in the set of micrographs from a given nerve. The standard deviation was then divided by the square root of the number of micrographs to give the error of the average number of axons per micrograph. This error term was multiplied by the ratio between the total area of the ultrathin section and the sample area, which yielded the standard error of the mean. Any systematic regional variation in the density of axon packing, as in the optic nerve of adult cats, would obviously result in an overestimate of the standard error calculated as described above. But we found that the packing density of fibers in the fetal optic nerve was comparatively homogeneous and for this reason the simple formula we have used is reasonably accurate.
†Percentage of growth cones depends on distance from the eye. Range from 2% to 100%.
§Not analyzed.
‡Estimate from this animal is accurate only to within ± 20% due to angle of section.
**Littermates.
††Littermates.
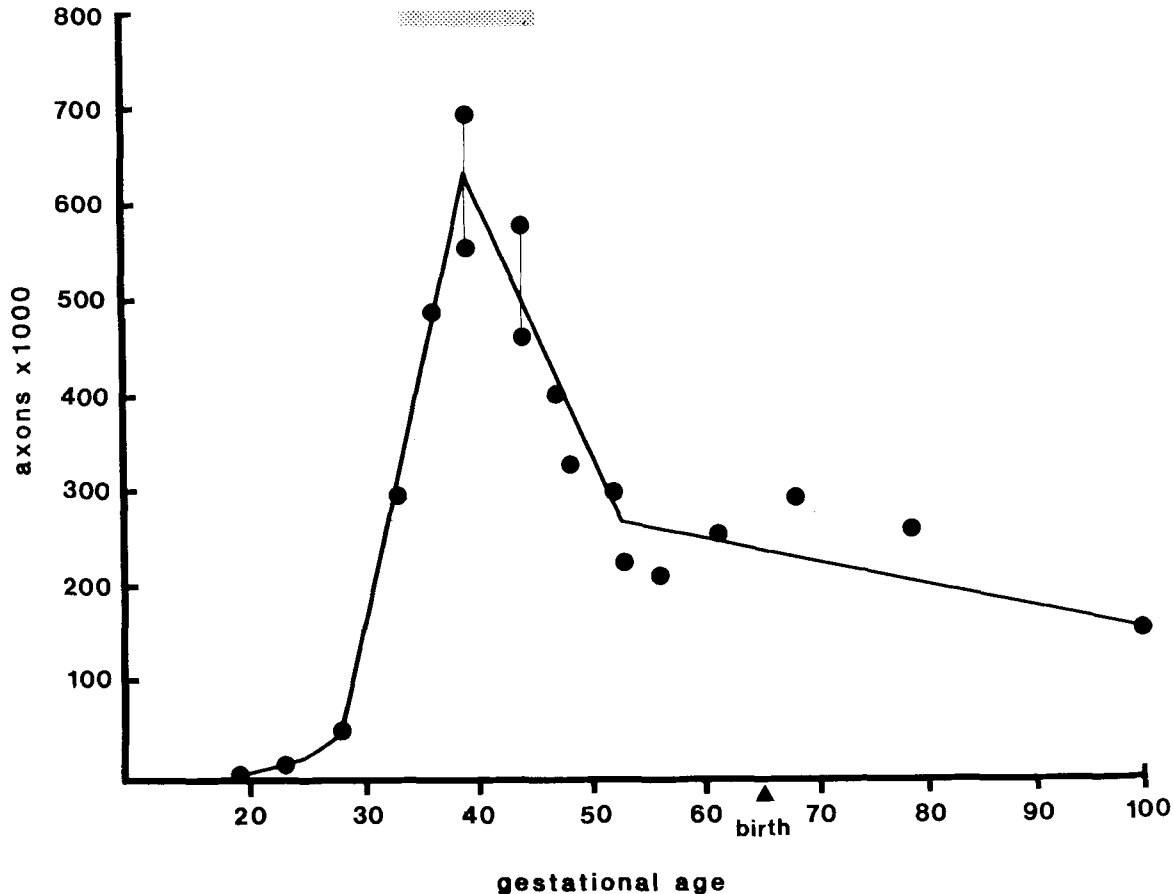
Fig. 1. Number of fibers in the optic nerve during development. Individual data points (see Table 1) are plotted as circles. The peak fiber number—560,000–700,000—reached at around E-39 underestimates total axon production by 100,000–200,000 since axons are lost before the peak is reached. The gray stripe above the peak therefore represents the approximate total axon production. The apparent rise in axon number from E-52 to P-2 is a sampling artifact. Fiber number in individual nerves actually decreases slightly during this time as demonstrated by the small number of necrotic axons in nerves during the perinatal period. The adult value is reached as early as the 100th day after conception, or about 36 days after birth.

Measurement of fiber caliber. The area and perimeter of 2,000 fibers in each nerve were measured with the aid of an image analysis system (Zeiss Videoplan), and the diameter of a circle with an area equivalent to that of each fiber was calculated and used to make histograms. Each histogram represents a uniform and unbiased sample of the transverse section. Profiles of large axons and growth cones are more likely to intersect the boundaries of micrographs than are those of small axons, and consequently their contribution and size will tend to be underestimated. To sidestep this source of error we placed a mask with a wide border over micrographs and measured the area of all axons completely within the central hole of the mask. The mask was then removed and the areas of those fibers that had initially intersected the margins of the mask were measured.

RESULTS

As is true of other parts of the central nervous system, the 12–18-mm-long optic nerve of the adult cat contains oligodendrocytes, astrocytes, and blood vessels, and is surrounded by a glial limiting membrane, a basal lamina, and meninges. In the adult cat there are 140,000–165,000 reti-

nal ganglion cells in each eye (Illing and Wässle, '81; Chalupa et al., '84) and a corresponding number of fibers in each optic nerve (Williams et al., '83, '85; Williams and Chalupa, '83b; Chalupa et al., '84).

The results are divided into three sections. The first deals with quantitative aspects of nerve development; the second describes the ultrastructure of the nerve during axon ingrowth, concentrating on the characteristics of ganglion cell growth cones; the third section summarizes our findings on fiber necrosis.

Quantitative aspects of nerve development

Rise and fall in fiber number. We determined the number of fibers in the optic nerve at 13 prenatal and 4 early postnatal ages (Table 1, Fig. 1). The word *fiber* is used here to include normal axons, growth cones, and necrotic axons. Axons of retinal ganglion cells enter the precursor of the optic nerve—the optic stalk—at the end of the third week of gestation. However, merely 88 fibers were counted in a midorbital section of the optic stalk taken from an E-19 embryo (Figs. 3, 4). But by E-23 there were nearly 100 times as many axons in a section of the nerve taken close to the eye, although remarkably, a section of the same nerve tak-
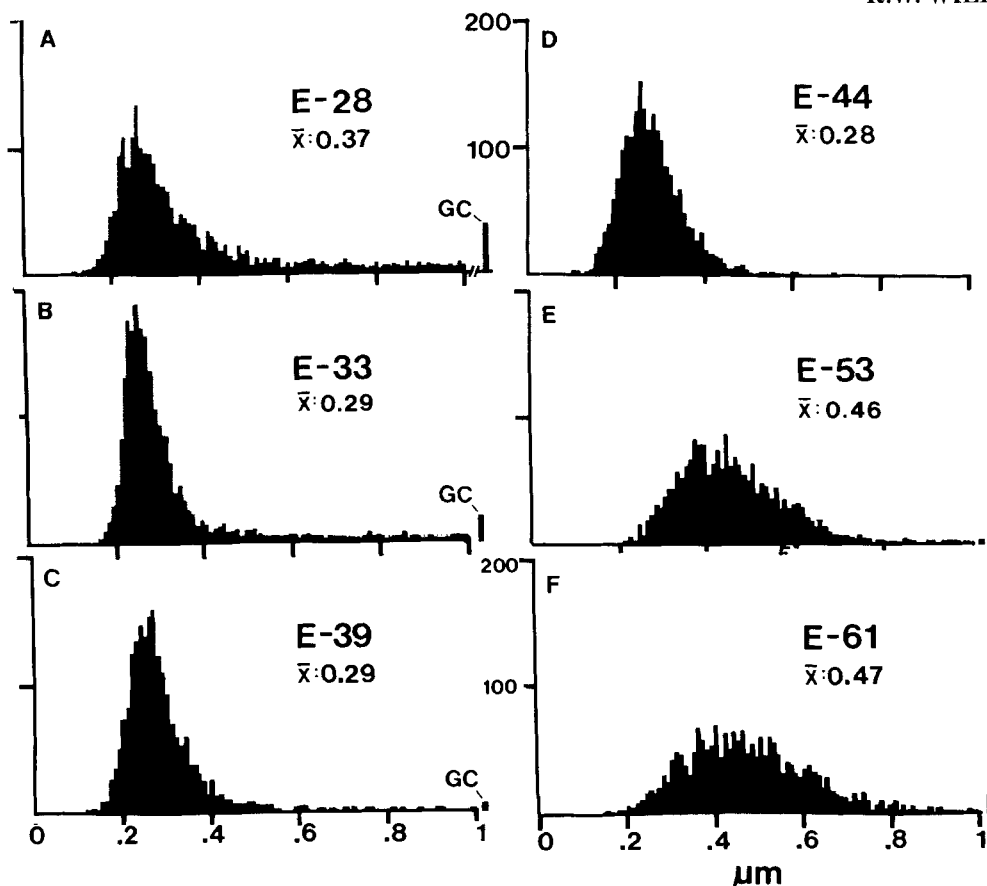
Fig. 2. Histograms of fiber size in the prenatal optic nerve of the cat. At E-28 (A) large axons contribute to the right-side tail of the histograms. The bin to the far right of histograms A–C represents growth cones (GC) with diameters above 1 μm. As early as E-33 the contribution of large axons is less pronounced (B), and as growth cones extend beyond the optic nerve at E-39 and E-44 (C,D) the large axon component disappears and as a conse-quence the average fiber diameter drops to about 0.3 μm. After E-48 (E,F), the mean diameter increases steadily, reaching about a third of the adult value when myelination begins at around birth. All histograms are based on 2,000 measurements distributed evenly across cross sections of nerves. In E and F the small overflow bins simply represent large axons.

en near the optic chiasm (Fig. 6) contained merely eight fibers, five of which were growth cones!

By E-28, 43,000 fibers have extended into the orbital part of the nerve (Table 1, Fig. 16). During the next 5 days the number of fibers increases rapidly—nearly 50,000 axons are added each day, and already by E-33 the nerve contains 292,000 axons, about twice as many axons as in the mature nerve. The number of fibers and their density of packing finally reaches a peak at E-39, nearly 3 weeks after the entrance of the first axons (Table 1): as many as 698,000 fibers are packed together at a density of 7.5 per 1.0 μm², twice the value at E-28 (Table 1). This high population is retained until E-44: two nerves of littermates at E-44 contained 580,000 and 454,000 fibers.

The substantial difference in the number of fibers—up to 23%—in nerves from littermates at E-44 and at E-39 (Table 1) concerned us. Was it real or did it result from inaccurate methods? To solve this problem a second ultrathin section was cut from the same E-44 nerve that we had estimated contained 457,000 ± 21,000 fibers. This second section, located 1 mm closer to the chiasm, contained 441,000 ± 28,000 fibers. The close agreement between these estimates indicates that the differences between littermates reflects individual variation rather than technical variability.

The number of axons in the nerve drops sharply between E-44 and E-53. Indeed, it is reduced to less than half its peak value: a nerve from an E-47 fetus contained 403,000 fibers, that from an E-48 fetus contained 328,000 fibers, that from an E-52 fetus contained 308,000 fibers, and that from an E-53 fetus contained 225,000 fibers (Table 1).

During the perinatal period, from E-56 through P-12, no consistent downward trend in axon number is evident: for example, a nerve from an E-56 fetus had as few as 230,000 fibers, whereas a nerve from a 3-day-old kitten had 293,000 fibers. However, given our results on the incidence of ne-crotic fibers in the nerve during this period (described on page 53), it is quite likely that the axon population in individual nerves does, in fact, decrease at a slow rate. By P-36 the number of axons in the nerve has reached a ma-ture value of 158,000, within the range we have encoun-tered in normal adult cats (Williams et al., '83, '85; Williams and Chalupa, '83b; Chalupa et al., '84).

The increase in axon caliber. In the optic nerve of the adult cat there is large variation in the caliber of the my-elinated fibers: the smallest axons are 0.2 μm in diameter (excluding the myelin sheath); the largest are 7.5 μm in diameter; but the overall distribution of fiber size in the
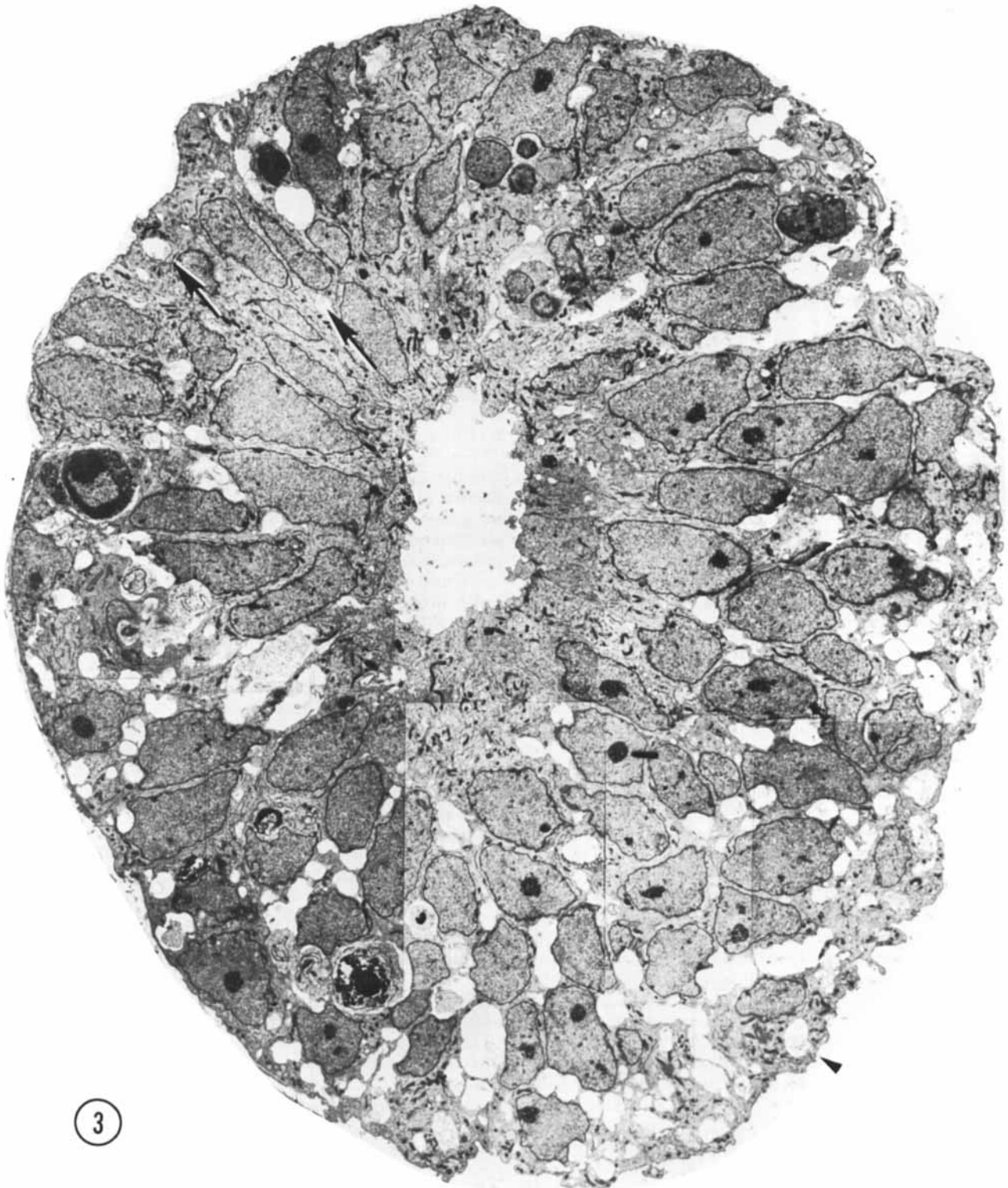
Fig. 3. The optic stalk—precursor of the optic nerve—at E-19. This section contains 86 axons and 2 growth cones (see Figs. 4–6). Most fibers are located in the lower, ventral part of the stalk in prominent extracellular ducts. Arrowhead marks the site of the growth cones reproduced in Figure 6A. Only a few axons are situated in the upper half of the stalk (arrows mark the axons shown in Fig. 5A,B). Necrotic cells, characterized by dispersed ribosomes, ruptured nuclei, and dark, mottled cytoplasm, are prominent at the 7-, 9-, and 11-o'clock positions. Processes of several necrotic cell partly fill ducts. At this age the lumen of the stalk (center) is still patent. Cells in the upper left portion of the figure extend radially the full width of the tube. In contrast, cells in the ventral portion of the stalk do not have a radial orientation. ×2,200.
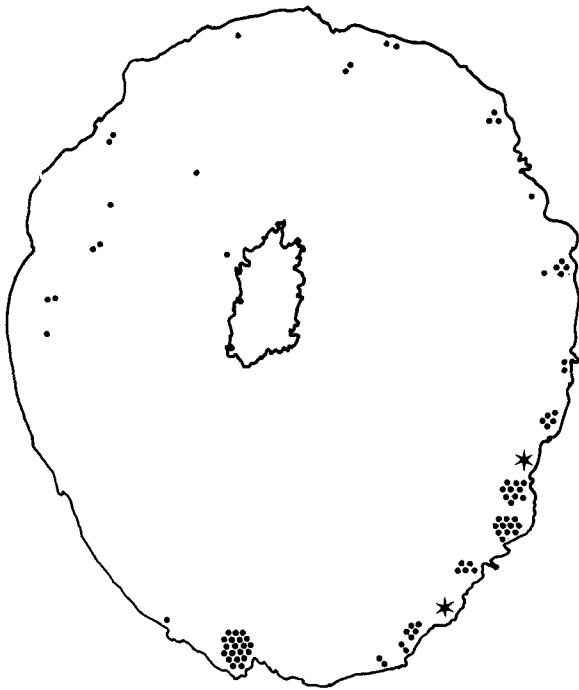
Fig. 4. Distribution of the first 88 fibers in the midorbital part of the optic stalk at E-19. The positions of axons are marked by small dots; growth cones are represented by stars.

mature nerve is bimodal with modes at about 1 and 2 μm (Williams and Chalupa, '83b; Williams et al., '85). Fibers are packed together at a mean density of 7 to 9/100 μm². By contrast, in the fetal cat all axons are unmyelinated, the distributionisstrictlyunimodal,andaxonsarepackedtogether at a density that at its peak is 100 times greater than in the adult nerve!

Based on histograms of axon caliber, the growth of optic fibers in the fetal cat was divided into three stages (Fig. 2). The first stage lasts from the onset of axon ingrowth until about E-28. The most striking feature of this period is that the nerve contains many large axons that make up a sizable fraction of the total fiber population and that contribute to an extensive histogram tail (Fig. 2A). These large axons are actually the long trailing parts of fibers located just behind growth cones, and as expected, the number of such large fibers at early ages is proportional to the number of growth cones. For instance, at E-28, 10% of all fibers have diameters above 0.6 μm and 2% of all fibers are growth cones with diameters above 1.1 μm (see page 49). By E-33 only 4% of axons are larger than 0.6 μm in diameter and there is a corresponding drop in the density of growth cones to about 1.0%.

The second period starts as early as E-33 and lasts until E-48. Growth cones and large axons, although still present in the nerve up until E-39, make up a comparatively small fraction of the total fiber population. The decrease in the fraction of growth cones in the nerve leads to a corresponding drop in the range and average size of fibers; mean fiber diameter decreases from 0.37 μm at E-28 to approximately 0.30 μm between E-33 to E-44 (Fig. 2B–E). The histograms also become more nearly symmetrical about their modes because of this loss of the rightward-extending "growth

cone" tail. The surprising feature of the second period is that there is no increase in fiber diameter: during this period, axons grow exclusively in length. However, even as early as E-44, before cumulative histograms of fiber diameter display any noticeable upward shift in axon diameter, there are both isolated instances of large axons and even a few collections of large axons (for example, those in the upper half of Fig. 22). Some of these may be the trailing ends of growth cones, but at least a fraction may simply be large-caliber axons.

The third period of growth begins as early as E-48, roughly concurrent with the onset of segregation in the dorsal lateral geniculate nucleus (Shatz, '83; Chalupa and Williams, '84, '85). At this age the diameter of axons increases steadily. Although the minimum diameter of optic axons remains about 0.2 μm, the range broadens considerably, peak values reaching up to 1 μm (Fig. 2F–H). No myelinated axons are present in the nerve at E-56, but by E-61 a small number of fibers are ensheathed by broad glial tongues (Fig. 24), and an even smaller number of fibers (96 out of 9,140) are surrounded by thin rims of compacted myelin. Three days after birth the nerve differs only in that the number of myelinated fibers, and the thickness of their myelin, is greater. By P-12 the nerve is much more mature in appearance (Fig. 25A); about 25% of the axons are myelinated, and another 30% are promyelinated axons in the process of receiving their first glial wraps. Associated with the onset of myelination, the optic fibers grows substantially; diameter increases rapidly from 0.5 μm at P-2 to 0.7 μm at P-12, and by P-84 mean axon diameter has already reached 1.7 μm, close to typical adult values (Williams and Chalupa, '83b). However, even as late as P-84 the bimodal distribution is not as pronounced as in adults.

Size and organization of fascicles. At E-28 each of the 100 fascicles in the nerve contains about 400 fibers. By E-33 the number of fascicles has increased to nearly 300, and each of these contains an average of 1,000 fibers (Fig. 15). Fascicles probably fuse with one another and split apart a great deal in the cat, as they do in monkey (Williams and Rakic, '85a) and mouse (Silver, '84), and thus the precise number of fascicles is likely to vary along the length of the nerve. Variation in the size of fascicles is substantial: the smallest contain 10 to 100 fibers and the largest contain more than 2,500 fibers (Figs. 7–9). The sevenfold increase in the total fiber population between E-28 and E-33 is associated with a threefold increase in the number of fascicles and a 2.5-fold increase in the number of axons per fascicle. Both central and peripheral fascicles grow considerably in size between E-28 and E-33, and the size of fascicles is not strongly related to their eccentricity at any age. This suggests that new fascicles are not simply added at the periphery of the nerve as successive waves of axons grow into nerve, because if this were the case, central fascicles would probably retain a relatively stable population of axons and the newest fascicles at the extreme periphery would be comparatively small.

Despite a 240% increase in the number of fibers between E-33 and E-39, the average number of fibers per fascicle rises merely 8%—from 1,000 to about 1,080. Naturally, the increase in the population of fibers is accompanied by a substantial increase in the number of fascicles. In comparison to the E-33 nerve that contains 289 fascicles, the E-39 nerve with the largest axon population contains 550 distinct fascicles, each set off from its neighbors by a glial partition 0.2–2.0 μm thick. Since new fibers grow into vir-
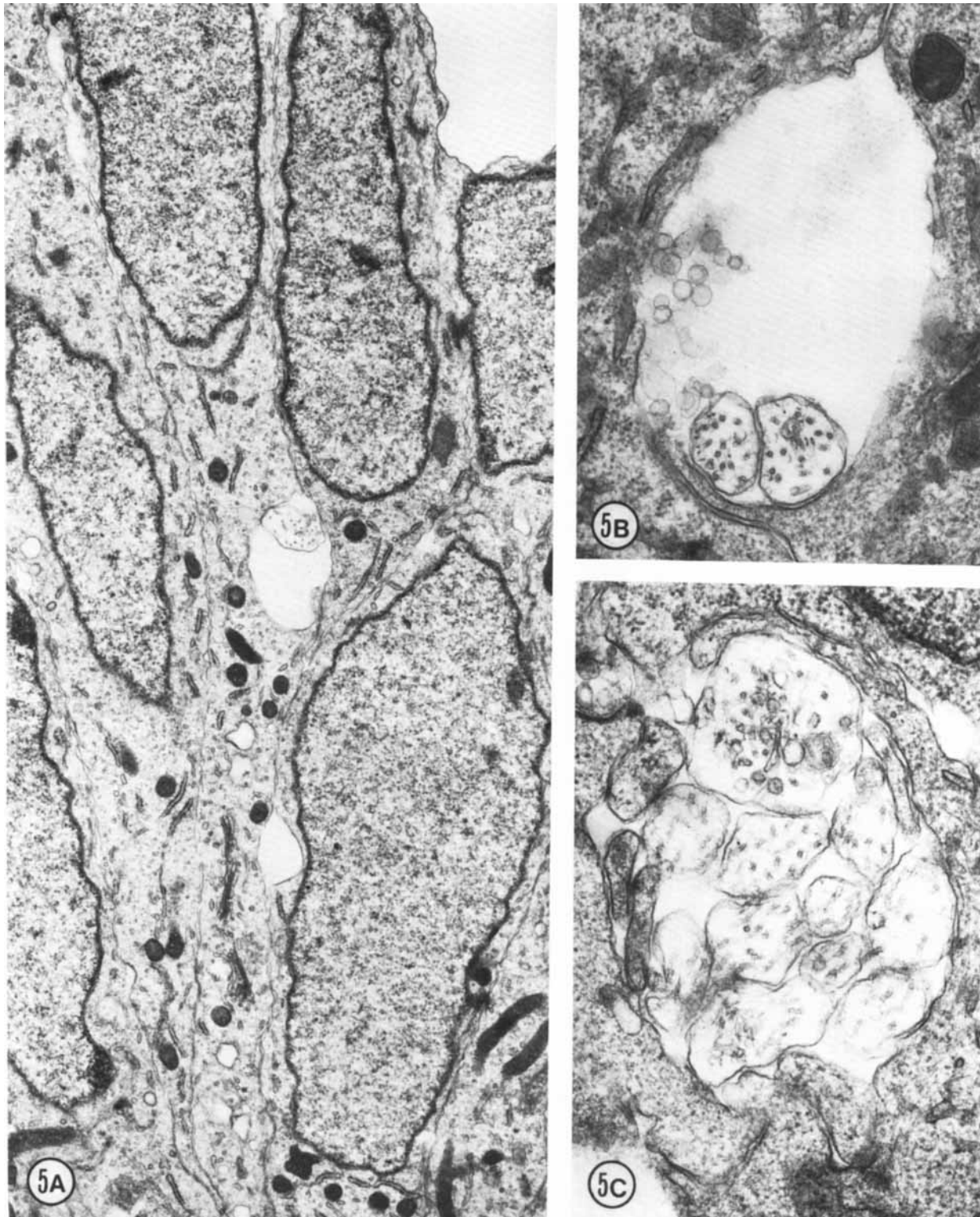
Fig. 5. The first axons in the optic stalk at E-19 A. Single isolated axon situated between radially oriented neuroepithelial cell processes in the optic stalk 12.5 μm from the edge of the nerve and about 11 μm from the lumen and the nearest axon. The site is marked by an arrowhead in Figure 3. ×12,800. B. Fascicle of two axons both of which contain neurofilaments. The loose vesicular material within the duct may be the remnants of a growth cone ruptured during fixation. Diameters of these axons are 0.39 and 0.46 μm. ×34,500. C. A tightly packed fascicle of 11 axons at the ventral periphery of the stalk. The large fiber that contains an abundance of tubu-lovesicular material and several neurofilaments is probably sectioned close to, or through, the core region of the growth cone. ×38,500.
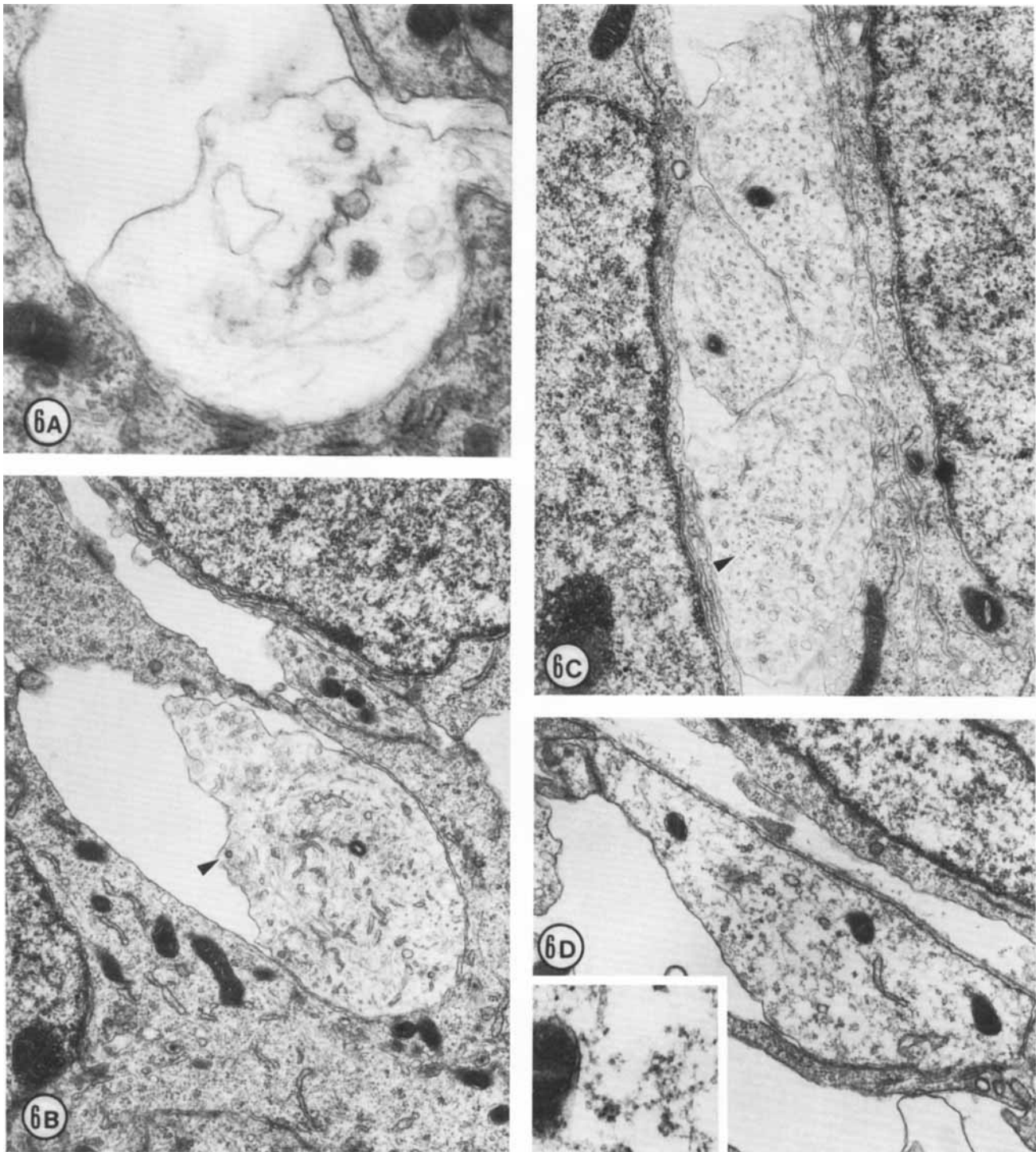
Fig. 6. Growth cones and neuroepithelial processes at E-19 and E-23. A. Growth cone at E-19 marked by an arrowhead in Figure 3. The first growth cones in the nerve are large and pale, and generally have few and very simple lamellipodia. This growth cone has a diameter of 1.6 μm and in this section contains no neurofilaments. ×36,500. B. Growth cone at E-23 with a diameter of 2.3 μm. Although this growth cone resembles that reproduced in A, it contains many neurofilaments and a large network of endoplasmic reticulum. Arrowhead marks a coated vesicle. ×20,000. C. Three-fiber fas-cicle. The diameters of these fibers are 1.6, 1.5, and 1.1 μm. The larger fibers are sectioned at or near the core of the growth cone (see text). A cluster of neurofilaments in the lower growth cone is marked by an arrowhead. ×24,000. D. Neuroepithelial processes apposed to the basal lamina. Although it resembles a large growth cone, it contains many ribosomes (see Inset), rough endoplasmic reticulum, and comparatively large mitochondria and thus is actually a neuroepithelial endfoot. ×20,000; inset ×65,000.
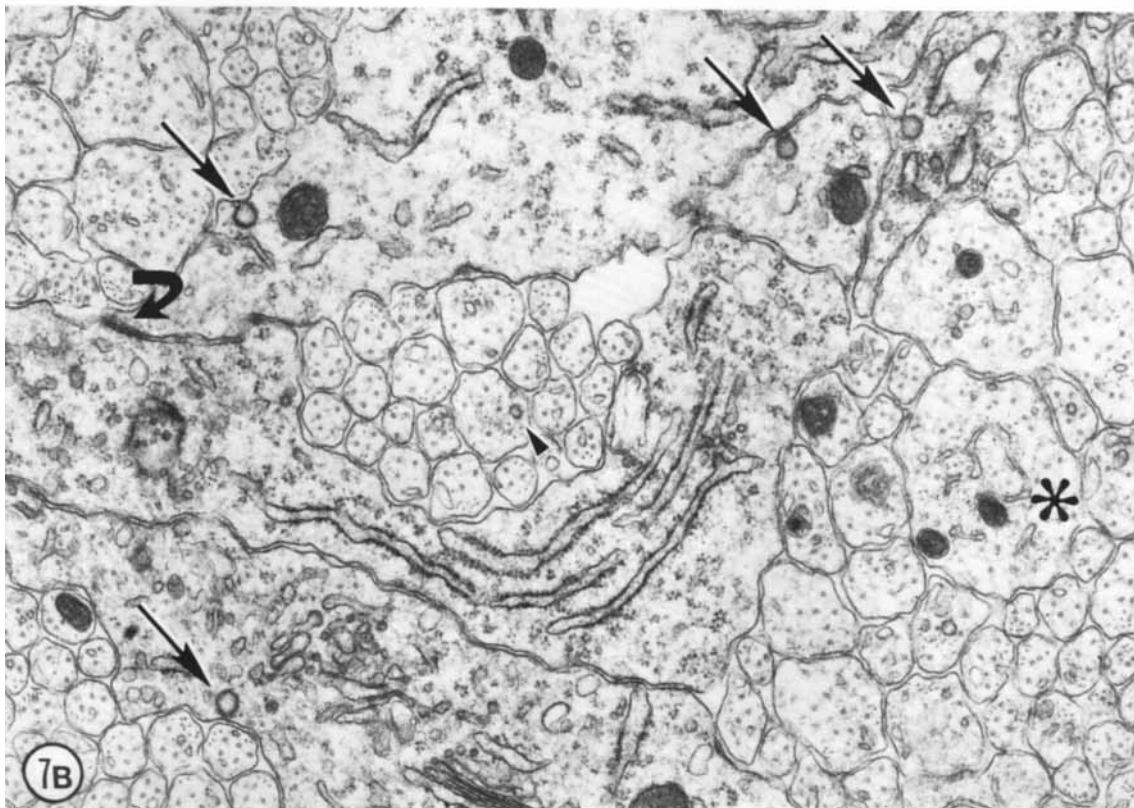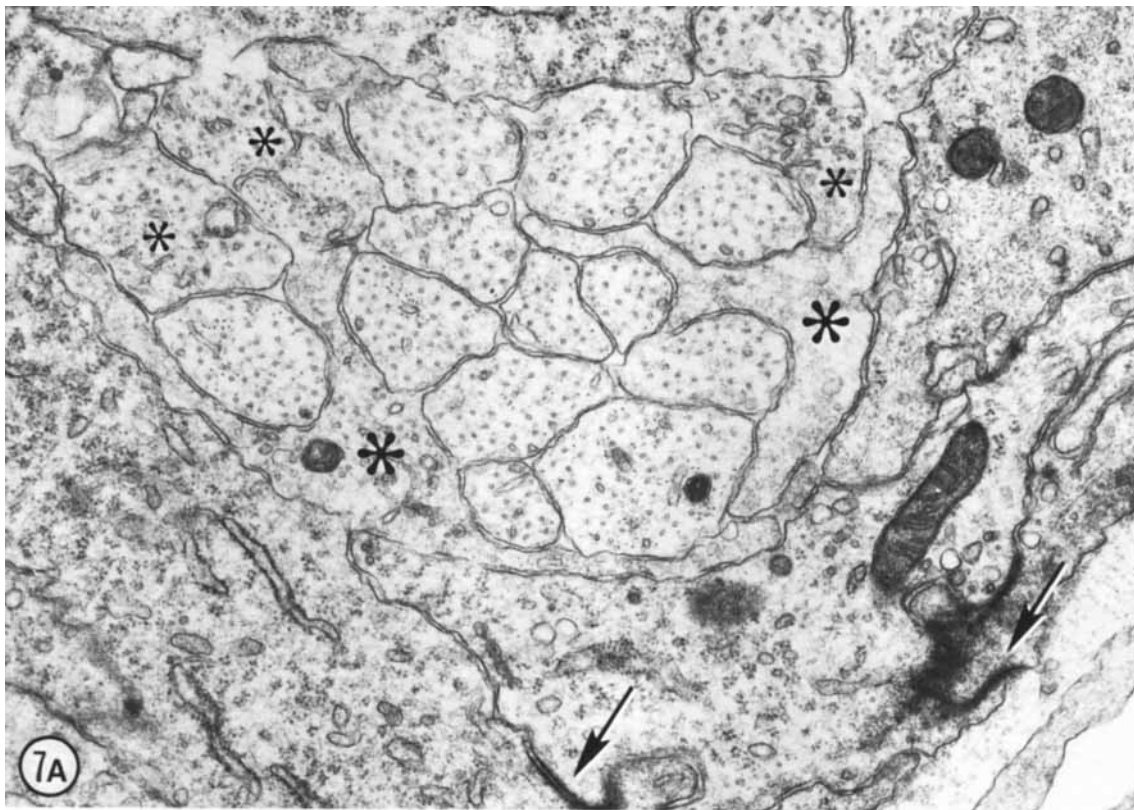
Fig. 7. Axons and growth cones at E-28. A. Fascicle at the nerve's periphery. Two growth cones with perimeters of 12 and 16 μm are sectioned through their lamellipodia (large asterisks). Another three growth cones (small asterisks) are sectioned through their cores. The remaining fibers in this fascicle, although not categorized as growth cones, are remarkably large (mean diameter is 1 μm) and contain many microtubules and neurofilaments. Large axons are probably cut close to their expanded tips. Note the difference in size of mitochondria in glial cells and in fibers and growth cones. Two electron-dense junctions between adjacent cells of the glial limiting membrane are marked by arrows at the edge of the nerve. B. Central fascicles of axons at E-28. The 22 axons in the very small ventral fascicle have an average diameter of 0.39 μm, about one-third the value of those in A. This field contains a single growth cone (asterisk) sectioned through or near the core. Axons in central fascicles are smaller and probably older. Neurofilaments tend to cluster close to the edges of fibers. One axon (arrowhead) contains a coated vesicle. As at the periphery, processes of glial cells are occasionally linked together by small junctions (bent arrow). Very large coated pits are common on glial cells (arrows). ×17,500.
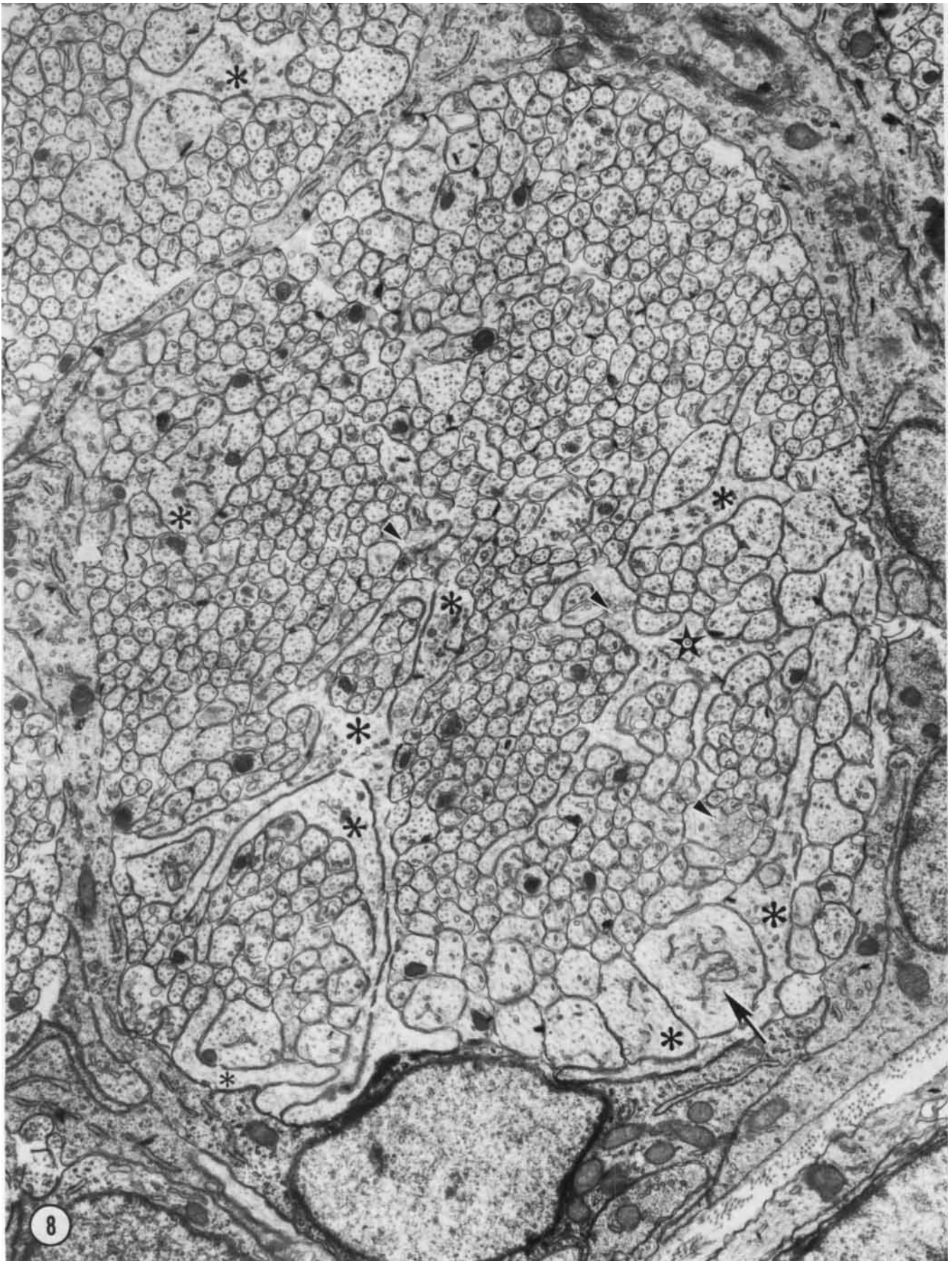
Figure 8

tually all fascicles even as late as E-33 (see the following section), the constant fiber population per fascicle between E-33 and E-39 suggests that the maximum size of fascicles is regulated in some manner by glial cells and their processes and that fascicles are repartitioned throughout the period of axon ingrowth.

Starting at E-44 the processes of glial cells extend into and subdivide axon fascicles (Fig. 23). Because fascicles are not as distinct as at earlier ages their number could only be approximated. Nerves taken from animals between E-44 and E-53 had 400–500 major fascicles (about the same number as at E-39), but each of these was split into at least two, and in some cases, as many as eight smaller compartments (Fig. 23). Glial proliferation and growth continue vigorously as late as P-12, and the mixture between glia and groups of axons is so thorough during the perinatal period that it is not even possible to approximate the number of fascicles.

Ultrastructure of the nerve during axon ingrowth

Optic stalk. From E-19 until at least E-23, the precursor of the optic nerve—the optic stalk—consists largely of neuroepithelial cells. Some of these cells are columnar and span the full width of the wall of the stalk (see the upper right quadrant of Fig. 3). Other cells appear to have lost their inner, luminal processes and to have moved toward the periphery of the stalk through which the first axons grow (see especially the lower half of Fig. 3). However, as early as E-23, the radial arrangement of neuroepithelial cells is no longer apparent. Adjacent lumenal (ventricular) processes of neuroepithelial cells are joined together by intermediate junctions up to 2 μm long. Their most characteristic feature is an extremely dense staining of the cytoplasm just beneath the cell membrane. In contrast, the peripheral ends of neuroepithelial cells are joined sporadically by small junctions that resemble, but are distinct from, punctae adherens described previously in a classic study of the meninges by Nabeshima et al. ('75, p. 131, their Figs. 21, 22). Frequently, however, no junctional specializations of any type are evident between the marginal ends of neuroepithelial cells (e.g., Fig. 5B).

One prominent feature of the optic stalk at E-19 and E-23 is the abundance of large, roughly circular intercellular spaces between the peripheral ends of neighboring neuroepithelial processes (Fig. 3). These spaces range in size from 0.5 to 6 μm, but typically have diameters of about 2 μm. Approximately 140 were counted in transverse sections through the E-19 stalk. The majority of these spaces or ducts do not contain any fibers or other cell processes, and ganglion cell fibers grow within an apparently undistinguished subset of ducts.[1]

Many cells of the stalk are necrotic at E-19 and E-23. In the single section reproduced in Fig. 3, several dying cells are visible, and when one takes into account the short

duration of necrosis—on the order of 3 hours (Glücksmann, '51; Hughes, '61; Senglaub and Finlay, '82)—it seems probable that a large proportion of cells in the stalk die over a short period. The appearance of these dying cells varies—some contain many lysosomes, autophagic vacuoles, heavily condensed chromatin or completely obliterated nuclei, and dense aggregates of dark, undefinable debris (compare with Chu-Wang and Oppenheim, '78a). Others contain less debris and have comparatively pale cytoplasm with dispersed ribosomes. In several cases normal neuroepithelial cells have sequestered debris of necrotic cells in large phagosomes.[2]

Ultrastructure of axons. The first axons in the optic stalk contain from three to ten microtubules, clear vesicles, irregular membrane profiles (probably cross sections of the smooth endoplasmic reticulum), and only limited amounts of microfilamentous material (Fig. 5). In comparison to fibers in older fetuses, the axoplasm of the first complement of fibers is only lightly stained (compare Fig. 5 with Fig. 24), in large measure because of the low concentration of microfilaments and neurofilament. Although points of contact between neighboring axons and between axons and neuroepithelial processes are common, we saw no evidence of membrane specializations, either gap junctions or desmosomes.

At E-19, fibers are distributed around the whole perimeter of the stalk (Fig. 4). Nonetheless, as in other vertebrates (Müller, 1874; Robinson, 1896; Silver and Sapiro, '81; Scholes, '81), most axons are located within the ventral half of the stalk and less than 5 μm from the outer margin. The mean distance between fibers and the edge of the optic stalk is merely 2.7 μm. Although the young optic axons are very close to the margins of the central nervous system, none are actually situated at the extreme periphery of the stalk, apposed to the basal lamina at either E-19 or E-23, or for that matter, at any later stage of development. Although several processes with pale cytoplasm similar to growth cones were in several instances apposed to the basal lamina (Fig. 6D), in every case when examined at high magnification they were found to contain numerous ribosomes and polysomes (inset to Fig. 6D) and were therefore actually endfeet of neuroepithelial cells. At E-19, ten axons

---

[1]Similar large intercellular spaces—or "intercellular lakes" to use the phrase of Silver and Robb ('79)—are prominent in the eye during early stages of axon elongation, and it has been argued that these spaces actually form an aligned system of ducts that guide or polarize the growth of axons (von Szily, '12; Ulshafer and Clavert, '79; Silver and Robb, '79; Krayanek and Goldberg, '81). More recently, it has been recognized that the channels actually form a maze rather than an orderly linear array (Suburo et al., '79; Silver and Sapiro, '81), and it therefore seems that their role with respect to fiber growth is permissive—not instructive.

[2]Von Szily ('12) demonstrated that a wave of cell necrosis sweeps through the optic stalk from the retina toward the brain in advance of the ingrowth of the optic axons. In our tissue several of the ducts in fact do appear to contain necrotic processes (Fig. 3) and for this reason we find von Szily's idea that the ducts are just holes left behind by dying cells plausible. However, whether, as von Szily suggested (p.84), ingrowing axons are attracted to necrotic debris, and whether the wave of necrosis serves to guide axon elongation, remains controversial, especially in view of the fact that necrosis is apparently rare in the optic stalk of *Xenopus* (Cima and Grant, '82; and see Tosney and Landmesser, '85).

Fig. 8. Axons and growth cones in a peripheral fascicle at E-33. This fascicle contains 752 fibers with an average diameter of 0.30 μm. Most growth cones (asterisks) have diameters greater than 1.3 μm. Growth cones with long lamellipodia are prominent in the lower, peripheral part of the fascicle. One growth cone with elaborate lamellipodia has a perimeter of 25 μm (star) and neighbors 58 fibers. The core region of a large growth cone (arrow) with a diameter of 1.7 μm contains a labyrinthine smooth endoplasmic reticulum (see Fig. 11). Vesicular aggregates found both in growth cones and axons are marked by arrowheads. Glial cells occupy almost precisely 25% of the nerve at this age: their cytoplasm is dense and contains numerous ribosomes and is easily distinguished from axons and growth cones. No glial processes intrude into the fascicle itself. The nerve is still entirely avascular at this age. ×13,600.
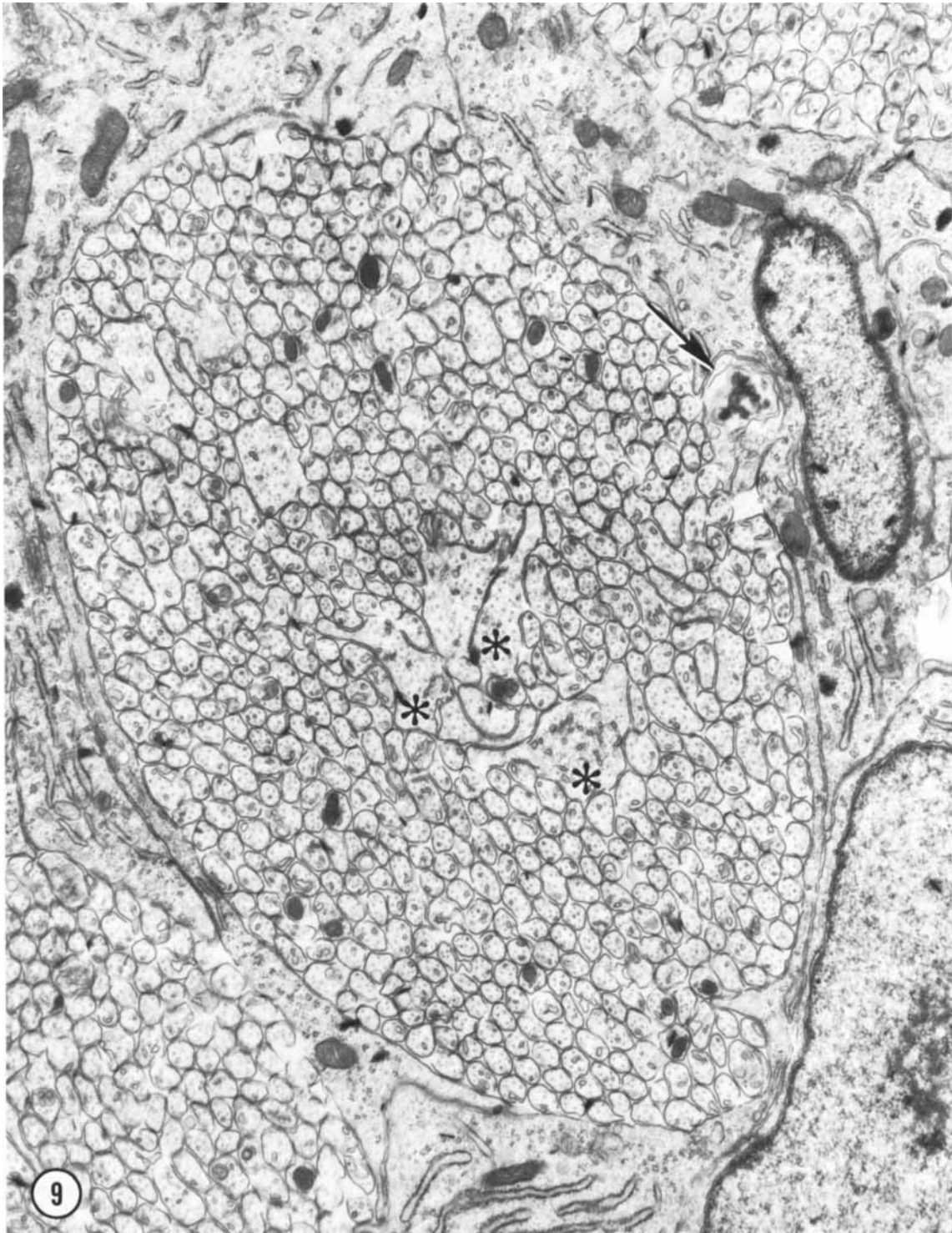
Fig. 9. Central fascicle at E-33 that contains 685 axons and three growth cones. Three growth cones are situated in the central part of this fascicle and at this level lack contact with glial cells. Arrow points to a necrotic axon. ×13,600.

Fig. 10. Longitudinal section of axons and growth cones at E-33. The edge of the nerve is shown in the lower left corner. The large growth cone in the middle of the field (asterisk) is at least 25 μm long. Microtubules in this growth cone are present to the left of the asterisk. The growth cone is probably extending in the direction of the large arrow. Coated pits (arrowhead in the upper-right quadrant), coated vesicles (arrowhead), and a dark core vesicle (small arrow) are common in axons as well as growth cones. ×18,400.

Fig. 11. Tubulovesicular mazes, probably part of the smooth endoplasmic reticulum, enmeshed in neurofilaments at E-33. These structures are common in the core region of growth cones (also see Fig. 7). ×43,400.

were located farther than 5 μm from the edge of the nerve, and in one extreme case, an axon was situated almost at the center of the stalk within 1 μm of the lumen.

Isolated small-caliber axons are found in the nerve at both E-19 and E-23 (Fig. 5A). The extension of growth cones is therefore almost certainly not contingent upon their proximity to other axonal surfaces. Similarly, the existence of axons deep within the wall of the stalk far from any other axons indicates that growth cones are able to penetrate between neuroepithelial cells and that they do not require contact with, or even proximity to, the endfeet of neuroepithelial cells. This result should be contrasted to the growth of fibers in the optic stalk of Xenopus in which it has been shown that axons are rarely if ever seen in isolation (Cima and Grant, '80, p. 232).

As early as E-28, a majority of axons contain neurofilaments (Fig. 7B). The mean number of neurofilaments per axon at this age is about six, but the range is large—from zero to 50. The density of neurofilaments in axons at this early stage of development surprised us because both Peters and Vaughn ('67) and Pachter and Liem ('84) have reported that optic axons of rats essentially lack neurofilaments until about a week after birth—an age roughly equivalent to E-50 in the cat. Perhaps neurofilaments are

quite labile during fixation early in development because the concentration of the heavy neurofilament subunit is so low (Willard, '83; Pachter and Liem, '84). In adult mammals, neurofilament polypeptides and microtubules are transported together at a rate of about 0.25 mm/day (Black and Lasek, '80). Since ganglion cell axons grow at rates of 1–2 mm/day (Rager, '80; Halfter and Deiss, '84) and possibly in spurts of up to 3 or 4 mm/day (cf. Schreyer and Jones, '82), and since neurofilaments and microtubules are prominent in growth cones as early as E-23 (see below), it is reasonable to conclude that the transport of these two cytoskeletal constituents is considerably faster early in development than at maturity (also see: Droz, '63; Grafstein and Murray, '69; Hendrickson and Cowan, '71).

Axon ultrastructure does not appear to change qualitatively during later stages of prenatal development. However, we found that for the last 12 days of gestation it was occasionally difficult to distinguish axons from small glial processes. The distinction between the two was based upon ultrastructure, form, and position. Many small glial processes do not contain ribosomes and at first inspection look like axons. Generally, however, glial processes are less circular than axons in cross section, are more frequently cut at oblique angles, contain a higher concentration of inter-

Fig. 12. Deep penetration of a growth cone (left) by a glial process (right) at E-33. A small uncoated vesicle (arrow) is forming within the lamellipodium directly under a glial process that contains several ribosomes. Based upon an analysis of serial sections this glial structure was club-shaped. ×41,000.

Fig. 13. Distribution of organelles in axons and a lamellipodium at E-33. The lamellipodium (asterisk) contains little other than microfilaments. As is generally true of osmicated tissue, these fibrils are not clearly organized. Microtubules within axons have a diameter of about 15 nm and the neurofilaments of 7–8 nm. Nearly all axons contain cross sections through smooth endoplasmic reticulum. Glial process to the far left (star) contains numerous ribosomes. In the center of the field is a large shaft of a growth cone that contains about 40 microtubules, a single mitochondrion, and smooth endoplasmic reticulum. Small unspecialized contact points between the lamellipodium, adjacent glia, and the large growth cone core are marked by arrowheads. ×84,000.
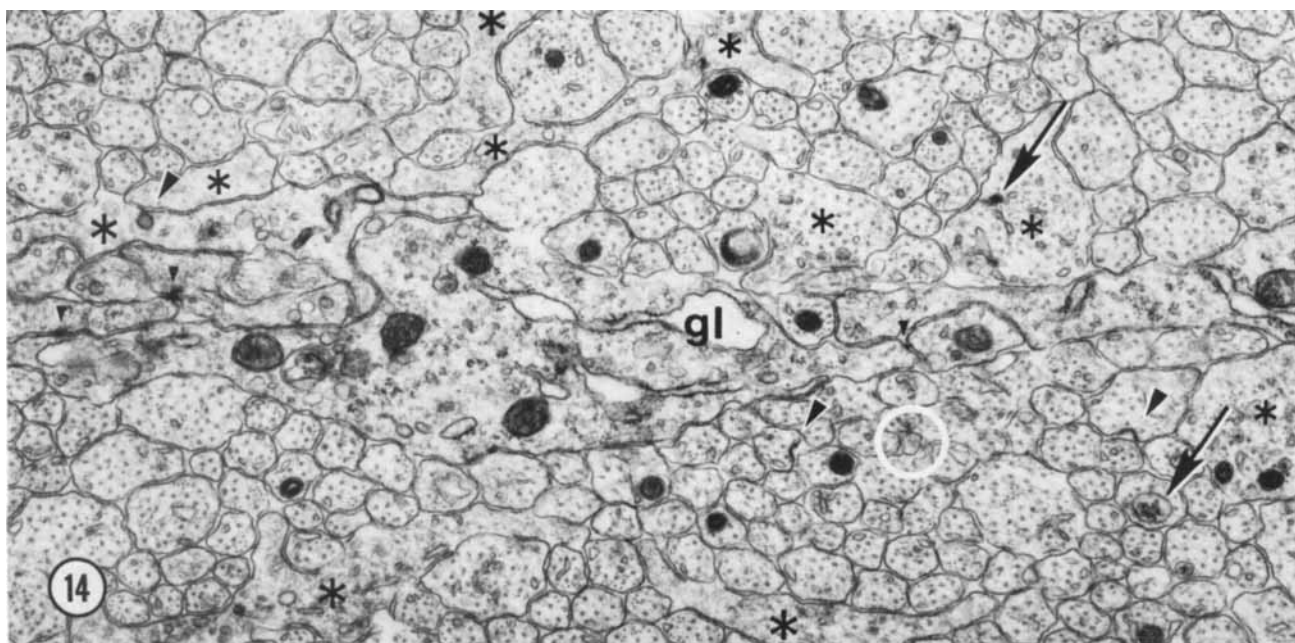
Fig. 14. Cytoplasmic organelles in axons and growth cones at E-28. Coated pits, marked by arrowheads, are shown forming on both a growth cone and two axons. The upper arrow points to a dense-core vesicle; the lower arrow to a multivesicular body. Very small arrowheads mark junctions between adjacent glia (gl). Asterisks mark growth cones and their lamellipodia. A single *fil*opodial profile is circled in white. ×15,000.

mediate filaments than axons do, and usually contain fewer than three microtubules (Fig. 24B). Axons typically contain a minimum of five microtubules. Only 5% of all processes presented a classification problem, and therefore we do not think that the accuracy of the counts was significantly degraded either by the inclusion of glia or the exclusion of axons.

Ultrastructure of growth cones. Growth cones of retinal ganglion cells are large, often have complex shapes, and possess an organellar composition that allows them to be readily distinguished from axons and glial processes (Figs. 7A, 8–13, 21). The important distinction between growth cones and glial processes is fortunately straightforward: a constellation of properties distinguish the two, the most absolute of which is the presence or absence of ribosomes. Axonal growth cones in the optic nerve in our experience never possess ribosomes, whereas glial pseudopodia contain a high density of ribosomes (Figs. 6–8). In this respect our results agree with those of Pfenninger and Bunge ('74). Another distinction is that mitochondria within the cores of growth cones are usually considerably smaller than those in glioblasts (compare the mitochondria in Fig. 7A,B). A final criterion, especially useful at later stages of development (ca. E-39, see Fig. 21), is the density of intermediate filaments: Density is high in glial processes and is much lower in axonal growth cones. These differences can be readily appreciated by simply examining the accompanying figures. The validity of these criteria has recently been confirmed in three-dimensional reconstructions of ganglion cell growth cones in the optic nerve of primate embryos (Williams and Rakic, '84; in preparation).

Axonal growth cones have two distinct parts: a distal fringe and a bulbous central core. The ultrastructure and shapes of these segments differ radically, and as a consequence, in single transverse sections through the optic nerve

growth cones display a range of characteristics that depend on how far from their tips they had been sectioned (Fig. 10).

The most distal parts of growth cones are made up almost entirely of sheetlike extrusions of membrane called lamellipodia. These have simple ultrastructure and contain merely a mesh of microfilaments and occasional clear and dense-core vesicles (Figs. 12, 16). Although microtubules, neurofilaments, and mitochondria are common within the core region of the growth cone (Figs. 7A, 10, 11), these organelles are almost entirely absent from lamellipodia. Lamellipodia are apposed either to the surfaces of glial cells, or to the other growth cones, or to axons. In single cross sections, the largest lamellipodia have a breadth of about 5 μm (Fig. 8), a thickness of 0.1–0.3 μm, and judged from growth cones sectioned longitudinally, they are up to 25 μm long (Fig. 10). The number of fibers growth cones are apposed to is in some instances remarkably high—up to 74 in single transverse sections. However, even growth cones in very small fascicles occasionally have very elaborate lamellipodia, and it therefore does not appear that the formation of lamellipodia is strictly related to the number of potential neighbors.

Filopodia—small, fingerlike protrusions extending out from growth cones—are surprisingly rare at all stages of development. At first sight it may seem that most of these outspread processes are small radial spikes (e.g., Fig. 8). However, in single longitudinal sections and in short series of transverse sections it quickly becomes apparent that these processes are virtually without exception sheets of membrane. If there are any filopodia, then in transverse sections they should appear as small oval profiles about 0.1–0.3 μm across their short axis containing microfilaments but no microtubules or neurofilaments (see, for example, the abundance of such profiles in Fig. 11 of Bastiani et al., '84). In a sample of micrographs of the E-28 nerve
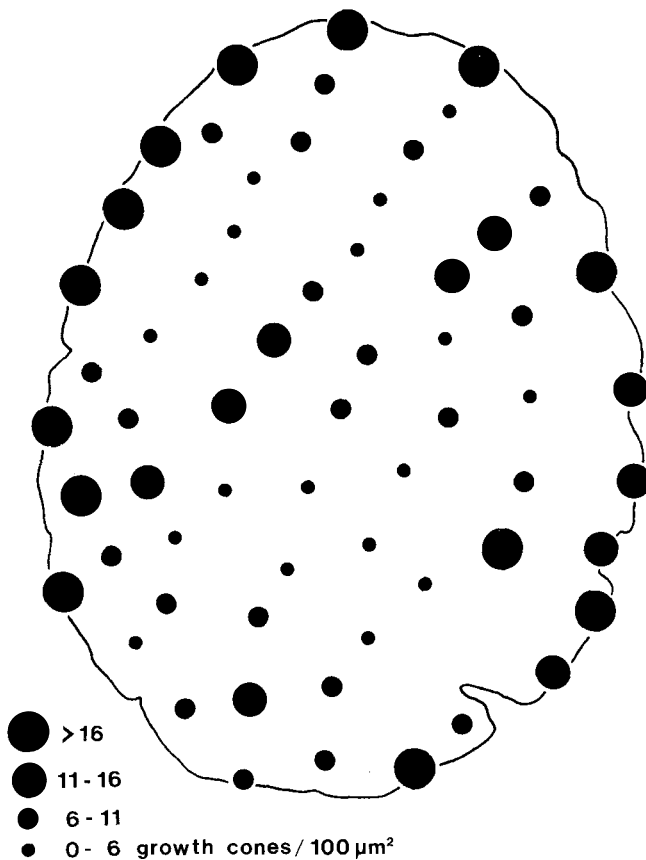
Fig. 15. Distribution of growth cones at E-33. Sixty-two micrographs, each covering 90 μm^2 of the nerve, were scored for growth cones. Corrections were made for the proportion of each micrograph containing glial processes and all calculations excluded regions occupied by glial cells and their processes (roughly 25% of the nerve at this age). The growth cone density per 100 μm^2 of nerve was split into four ranges; a high range (>16 growth cones/100 μm^2) is represented by the largest spots (the average for this group was 22 per 100 μm^2 and the highest value was 28 per 100 μm^2). Spots that actually interrupt the outline of the edge of the nerve represent micrographs taken at the extreme periphery. The smallest spots represent regions containing fewer than six growth cones/100 μm^2.

that contained 20,000 axons and about 400 growth cones, only 15 such presumed filopodial profiles were found (Fig. 15).

The core region of the growth cones from which the lamellipodia originate usually has a caliber three to five times greater than a typical axon (Figs. 7, 8, 11) and contains a great variety of organelles, including 40–60-nm clear vesicles, coated vesicles, coated pits, dense-core vesicles, mitochondria, microfilaments, a substantial amount of smooth endoplasmic reticulum, microtubules, and neurofilaments. All of these organelles are also found in axons, although in lesser numbers and in differing concentrations. For instance, the core region of growth cones often contains in the neighborhood of 15 microtubules and occasionally twice this number are noted in single sections. In comparison, the mean number of microtubules in typical axons with diameters ranging from 0.3 to 0.4 μm is five to six. The only structure seen exclusively in growth cones is a maze of tubules or membrane sacks resembling smooth endoplasmic reticulum that is usually enmeshed in a nest of neurofilaments (Fig. 11). The cisternea are more darkly stained than is typical for perinuclear endoplasmic reticulum.

Although nearly all growth cones have certain features in common, there are nonetheless several notable qualitative differences in their form and ultrastructure. In large part, this is due to sectioning growth cones at different distances from their tips. However, some differences appear to be age-related. At E-19 and E-23, growth cones in the optic stalk have only a small number of stubby protrusions, which do not seem to merit either the term lamellipodia or filopodia (Fig. 6A–C). With a few exceptions, the form of these first growth cones appears to be particularly simple. Furthermore, the concentration of cytoskeletal components, particularly microfilaments, appears substantially less in this first group of growth cones than in those at E-28 and E-33.

Bastiani and Goodman ('84) have shown that in embryonic grasshoppers, filopodia of certain growth cones selectively penetrate into the core of other growth cones and induce the formation of coated pits. They have suggested that coated pits and vesicles mediate fiber-fiber recognition and perhaps ultimately the direction of axonal growth. Given this result, and the earlier work of Altman ('71) and Vaughn and Sims ('78) in which coated vesicles were linked with early stages of synaptogenesis, we decided to examine the distribution of coated pits in a large sample of fibers at E-28. We found that nine of 410 growth cones (2.2%) had prominent coated pits with diameters of 50–90 nm on their surfaces (Fig. 14). In addition, similar coated pits were also found on the surfaces of 30 (0.14%) out of 20,400 axons (Fig. 14). After correcting for the four- to fivefold greater perimeters of growth cones, we conclude that coated pits are about four times more common on growth cones than on axons. The direction of movement of these coated pits and vesicles is not known. However, the long necks connecting the main body of the coated pit to the surface suggests strongly that at least some are pulling away from the plasma membrane.

Although we found no evidence that neighboring growth cones ever had processes that protruded into one another (Bastiani and Goodman, '84; Tosney and Landmesser, '85), we did note two cases in which glial cell processes indented or deeply penetrated the surface of growth cone lamellipodia. In both cases, one or two 50-nm vesicles were found fused with the plasmalemma of the growth cone at these sites of intimate contact (arrow in Fig. 14) suggesting that some inductive event, perhaps similar to that described by Bastiani and Goodman ('84) between growth cones in the grasshopper embryo, is taking place. Examination of serial sections revealed that the glial intrusions were spines rather than ridges.

Number of growth cones. At E-28, 2.0% of all fibers are growth cones. They have perimeters between 3 and 6 μm with a mean of 4 μm—about four times that of axons. By E-33 the percentage of growth cones has dropped to approximately 1.1%. Their perimeters are on average slightly larger (about 15%) than those at E-28, and although the percentage of growth cones in the nerve is higher at E-28 than at E-33, the total number of growth cones actually peaks at E-33; nearly 3,000 are distributed in a nonuniform fashion (see below) throughout the nerve.[3] An additional 4–

---

[3]It should be noted, however, that since growth cones often have bifurcating lamellipodia in the optic nerve of embryonic primates (Williams and Rakic, '84), these percentages probably overestimate the total number of growth cones.

Fig. 16. The optic nerve at E-28; montage of low-power electron micrographs. At E-28 midorbital sections of the optic nerve have an elliptical shape with axes approximately 100 and 150 μm long. In transverse section the processes of glial precursors divide the nerve into clearly delimited fascicles of axons (Figs. 7, 16). At this level the nerve is made up of 105 fascicles that collectively contain approximately 42,000 axons and 800 growth cones. Peripheral fascicles are only slightly smaller on average than those at the center but contain fewer fibers and about twice as many growth cones. Growth cones are scattered widely. Remarkably few glial processes intruded within the fascicles themselves. The figure is reproduced at about one-half the magnification as the E-19 optic stalk (Fig. 3). The remarkable transformation in nerve architecture is evident. Neuroepithelial cells are no longer present, a distinct glial limiting membrane insulates the fibers, glial cells are dispersed throughout the nerve, and no remnant of the lumen is visible. At this age the nerve is avascular. ×1,250.
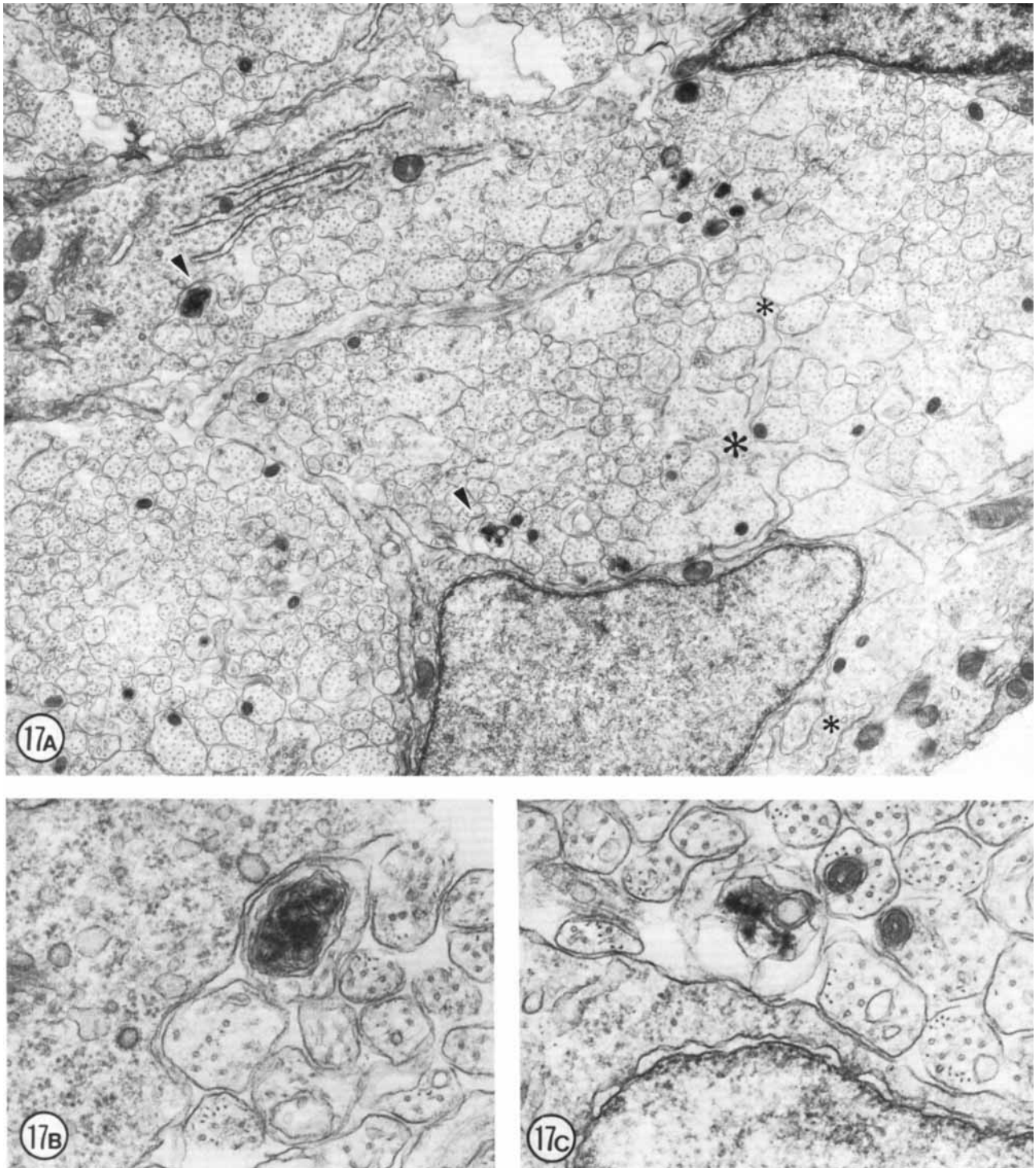
Figs. 17. Dying fibers in the optic nerve at E-28. A. A peripheral fascicle that contains dying axons (arrowheads). Their axoplasm is dark and membranes appear to be disintegrating. The ultrastructure of the majority of axons and growth cones (asterisks), however, is normal. ×11,300. B. Necrotic axon marked in A at ×43,000. C. Disintegrating axon marked in A at ×43,000.
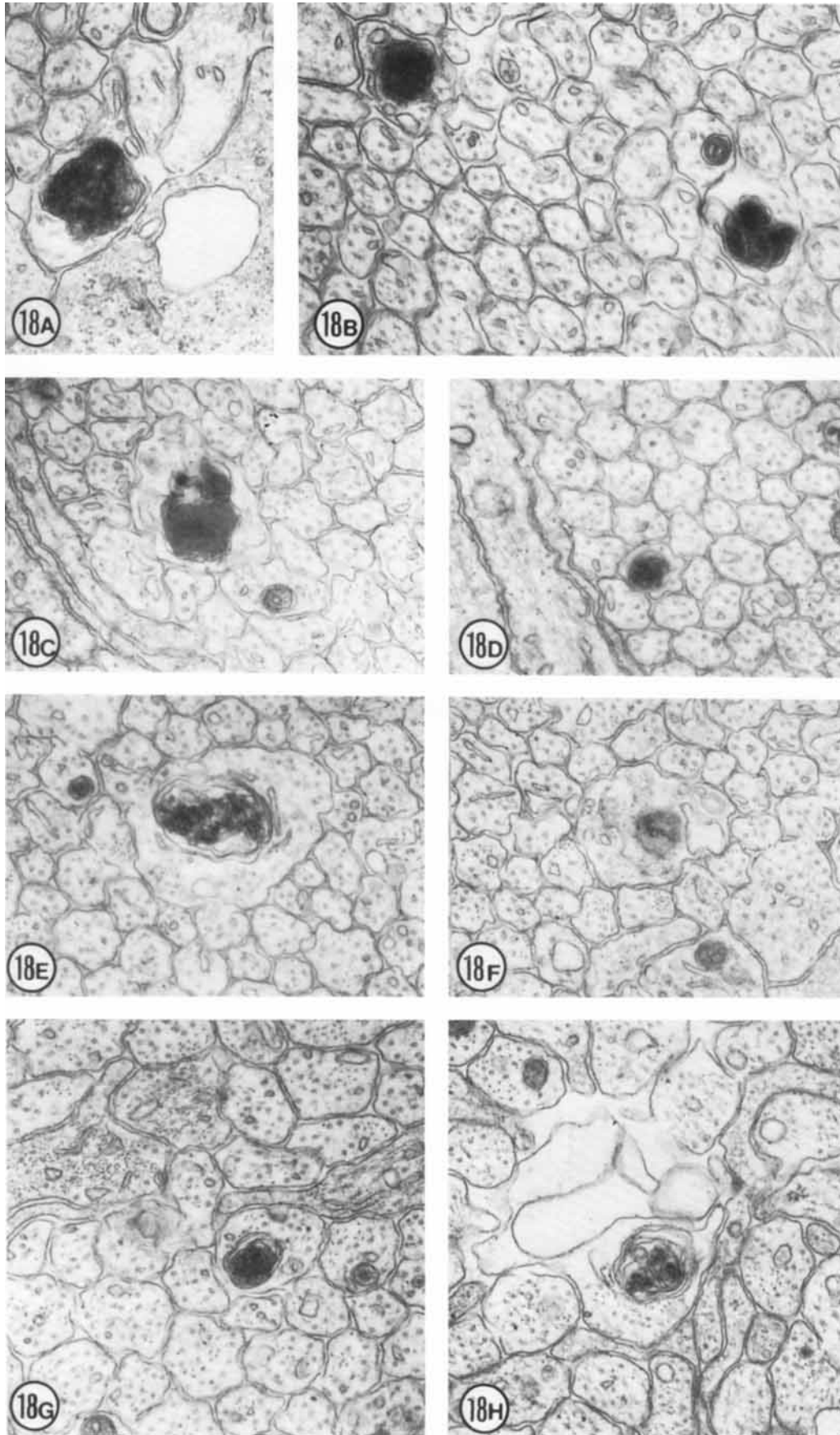
Figure 18

10% of all axons are unusually large (diameter > 0.6 μm) at these ages (Figs. 2A, 7A, 8). Since these large axons disappear with the same time-course as do growth cones they are almost certainly cross sections through the long, flared shanks of growth cones. By E-39 merely 0.2–0.4% of all fibers are classified as growth cones (Table 1), and these appear to be as large and complex as growth cones at E-28 and E-33. For example, the remarkable growth cone reproduced in Figure 21A has a span of 10.2 μm, a perimeter of approximately 40 μm, and makes contact with 42 axonal neighbors in a single transverse section. By E-44 there are essentially no growth cones in the nerve. One of the E-44 nerves was completely devoid of growth cones, whereas the other contained a total of less than 20 growth cones.

Distribution of growth cones. There is a moderate central-to-peripheral difference in the proportion of growth cones at E-28 and E-33 (Fig. 15). At E-28 there are twice as many growth cones at the nerve's periphery, within 12 μm of the margin, as there are at the center—ten versus five per 100 μm². By E-33, the absolute proportion of growth cones has decreased and the difference between center and periphery is only slightly more pronounced: densities remain about 5.0 per 100 μm² at sites located farther than 10–15 μm from the edge (7.2 per 100 μm² if glial processes are excluded), but are three- to fourfold greater at the edge (Fig. 15). Growth cone density reaches a plateau within 10 or 20 μm of the edge of the nerve, and consequently within central and pericentral parts of the nerve the density of growth cones shows little or no systematic change (Fig. 15). Virtually all central fascicles contain several growth cones.

At a local, fascicular level of analysis there often appears to be a slight central-to-peripheral gradient. Growth cones are somewhat more frequently located at the outer edges of fascicles, positioned between other fibers and glial processes (Fig. 7A). However, there are certainly numerous exceptions; many growth cones are found buried among axons in the center of large fascicles without evident glial contact (Fig. 7B).

At E-39 there is still a clear spatial gradient in growth cone distribution. Between 70 and 80% of the growth cones are located in a 50-μm-wide annulus of the nerve that covers half the cross-sectional area. The remaining 20–30% are situated more than 50 μm from the nerve's edge (Fig. 22B). In contrast to earlier ages, at E-39 substantial parts of cross sections of the nerve are almost completely devoid of ingrowing fibers. This is true not only of central regions, but also of fairly large peripheral sectors. The overall central-to-peripheral gradient of growth cone distribution may reflect the rough central-to-peripheral gradient in the generation of ganglion cells across the retinal surface (Walsh et al., '83), or as suggested by Bohn et al. ('82) and Silver and Rutishauser ('84), this may simply reflect a tendency for growth cones to grow close to the outer margins of the optic nerve.

Fiber necrosis

Early axon necrosis. As early as E-28, fibers that contain dark inclusions, dense lamellar structures, dilated and

very electron-dense mitochondria, large vacuoles, and disrupted plasma membranes are regularly encountered in the nerve (Figs. 17, 18A,B). Such a constellation of features is associated with acute stages of axonal disintegration during normal development in many parts of the nervous system (see Discussion). Some of the necrotic axons simply contain large electron-dense autolytic inclusions (Fig. 18A) that in many cases may be necrotic mitochondria or lysosomes (Webster, '61). Others show more severe signs of degradation: the entire axoplasm is dark and mottled, microtubules and neurofilaments cannot be resolved, and the axolemma is ruptured (Fig. 17B,C). The size of degenerating axons is variable, but in general they are about twice as large as their neighbors.

The percentage of necrotic axons is high at E-28—about 0.23%. At E-33 and E-36, only about 0.10% are obviously necrotic. In none of the nerves was there any strong evidence of regional differences in the proportion of dying axons—central, intermediate, and peripheral parts of the nerve contained roughly the same percentage.

There are also a number of axons that are abnormal in some ways, but not so strikingly abnormal as to enable us to confidently categorize them as necrotic. Such ambiguous fibers are not included in counts of necrotic axons. They may represent early stages of necrosis or they may be axons that have taken up the debris of other neighboring necrotic axons. Their numbers varies roughly in proportion to the number of axons that are unambiguously necrotic.

There are many necrotic axons in the nerve several days before retinal fibers can be demonstrated in the dorsal lateral geniculate nucleus with the aid of anterograde tracing methods at the light level (ca. E-32, Shatz, '83). This raises the intriguing possibility that some fibers die while still extending through the nerve. We therefore decided to search for necrotic *axon terminal bulbs* (Lampert, '67)—the equivalent of necrotic growth cones (Yamada et al., '71). The entire cross-sections of the E-28 and E-33 nerves were scanned at high magnification ($\times$20,000–30,000). Only five large necrotic fibers, that may have been the swollen ends of degenerating axons were found at E-28, but at E-33 nearly 20 extraordinarily large necrotic fibers and highly atypical growth cones were found (Figs. 19, 20). In every case, these structures are clearly not of glial origin: they never contained ribosomes, rough endoplasmic reticulum, or the large mitochondria characteristic of glial cells. Several of these necrotic fibers have features intermediate between growth cones and necrotic axons (Fig. 19). Some are extraordinarily large, even in comparison with growth cones, and contain regions almost exclusively occupied by bundles of neurofilaments (Fig. 19B–D). These fibers appear essentially identical to previous descriptions of reactive and dystrophic axon terminal bulbs described in the adult nervous system (e.g., Lampert, '67).

The period of heavy axon loss. An average of about 0.3% of axons in the optic nerve are necrotic between E-39 and E-48. The characteristics of necrotic axons during this period (Fig. 18E,F) do not differ in any respect from those described in the previous section at earlier stages. There do not appear to be any consistent spatial gradients in the location of necrotic axons. They are scattered throughout the nerve. By E-53 their incidence is quite low, less than 0.05%—and similar low values are found as late as P-2.

In order to calculate the total production of axons it was necessary to estimate the number of axons lost early in development while other fibers were still extending through

Fig. 18. Necrotic axons. A,B: E-33; C,D: E-39; E,F: E-53; G,H: E-61. Axons were counted as necrotic if they contained dark and mottled axoplasm. Most axons, such as those in B, C, and H, are partly disintegrated whereas others contain large accumulations of dense material (A, B, D). Other axons (i.e., G) are partly intact and the dense inclusions may either be necrotic mitochondria (a characteristic of early stages of degeneration) or may be debris that these axons have phagocytized. $\times$30,000.

the nerve. We estimated this number by first determining the time required to clear away the debris of dying axons during the period when all changes in the total fiber number can be attributed to fiber loss; that is, after all growth cones have grown through the nerve. Over a 216-hour period between E-39 and E-48 approximately 375,000 axons are eliminated. Thus an average of 1700 axons are lost per hour during a period when the fraction of necrotic axons makes up about 0.3% of the fiber population. Naturally however, more fibers are actually eliminated per hour at E-39 and E-44 than at E-48. It was therefore necessary to correct for the severity of axon loss at each age bearing in mind the total number of axons in the nerve. *The ratio of the number of necrotic axons in single cross sections through the nerve to the number lost per hour gives an estimate of the time required to clear away axonal debris of about 1 hour.* For comparison, the clearing time of the cell bodies of retinal ganglion cells has been estimated to be 2–4 hours in neonatal hamster (Sengelaub and Finlay, '82) and about 3 hours in the spinal cord of *Xenopus* tadpole (Hughes, '61). Using our 1-hour approximation, we estimate that between E-28 and E-39 from 0.09% to 0.26% of the fiber population is eliminated every hour (see Table 1). Subtracting the daily loss while correcting for differences in the incidence of loss at each age reveals that about 150,000 axons are lost between E-28 and E-39. We stress that this number is only a rough approximate because the number of individuals on which the calculation is based is low and because it is possible that clearing time varies as a function of age or even time of day (see Vogel, '78).

Late stage of axon loss. There are very few necrotic fibers in the optic nerve during the perinatal period. In fact, in the group of micrographs used to estimate total axon number at E-61 there were only two unmyelinated necrotic fibers among about 7,700 that were counted. Thus, the percentage of necrotic fibers is under 0.05%. However, at E-61 there are several necrotic glial cells (Fig. 24A). This wave of glial necrosis is probably related to the proliferation of oligodendrocytes, and it is tantalizing to speculate that even glia are overproduced during development (cf. Mori and LeBlond, '70; Hildebrand'71). Three of these necrotic glia were found within a sample of the nerve that covered merely 3.5% of its area. These observations are remarkably similar to those of Chu-Wang and Oppenheim ('78b), who previously described the necrosis of Schwann cells during the myelination of the ventral roots of the chick embryo.

By postnatal day 12, in agreement with Moore et al. ('76), about 25% of the fibers are myelinated. These fibers are generally considerably larger than nonmyelinated or promyelinated axons (Fig. 25A,B). It was of interest to determine whether, as suggested by Rager ('80) and Sefton and Lam ('84), necrosis is limited to smaller unmyelinated axons. In a sample of 15,000 axons, about 25 necrotic *myelinated* axons and three necrotic *unmyelinated* axons were found. The necrotic myelinated fibers had extremely dense axoplasm often full of intermediate filaments (Fig. 25C). In comparison to the perinatal cats (E-61, and P-2), the incidence of necrotic axons at P-12 is high. This observation makes sense because the clearing time for a myelinated axon is much longer than that of a naked axon—on the order of weeks and months (Nathaniel and Peese, '63; van Crevel and Verhaart, '63; Cook and Wiśniewski, '73), and this may explain the fact that necrotic axons are seen in

the nerve of the older kittens (P-36 and P-84), even though the population of fibers has reached adult levels. We are not the first to demonstrate dying myelinated axons in the kitten's optic nerve: Cook et al. ('74) reported that 3–5% of myelinated axons at P-7 showed degenerative changes but that by P-35 less than 1% showed similar evidence of necrosis. We counted far fewer necrotic axons in our P-12 and P-36 nerves. Possibly our criteria are more stringent. In any case, it is evident that both unmyelinated and myelinated axons undergo degeneration during normal development. This is also the case in the ciliary nerve (Landmesser and Pilar, '76), the trochlear nerve (Sohal and Weidman, '78), and the ventral roots (Chu-Wang and Oppenheim, '78b). Clearly, the hypothesis advanced by Sefton and Lam ('84, p. 115) "that axons lost during periods of cell death in any system will prove to be unmyelinated" is not tenable.

DISCUSSION
Synopsis

We have shown that a total of 800,000–900,000 axons grow into the optic nerve of the cat between E-19 and E-39. At the peak of axon ingrowth (E-28 to E-33) several thousand growth cones are distributed throughout the nerve, preferentially around the periphery but also within its core. Surprisingly, during this period of axon ingrowth numerous necrotic fibers are found throughout the nerve. However, the number of necrotic fibers does not peak until about E-44. A total of 80% of all axons are lost over a protracted period that begins about the same time fibers reach their targets (E-28), extends through birth (E-65), and lasts several weeks after eye opening.

Growth cones in the optic nerve

Identification of growth cones. The growth cones we have studied in the cat's optic nerve are similar in shape and ultrastructure to large velamentous axonal growth cones first described in detail by Skoff and Hamburger ('74). These authors analyzed serial sections of embryonic chick spinal cord and provided a thorough set of criteria by which to distinguish axonal growth cones from dendritic growth cones and growing neuroepithelial or glial processes. We have relied upon their criteria extensively. Our description is also generally in agreement with several recent electron microscopic studies in which retinal ganglion cell growth cones were reconstructed (Bodick, '80; Easter et al., '84; Williams and Rakic, '84, '85a). Perhaps the only notable difference is that Bodick ('80) reported numerous filopodia—he called them *microspikes*—extending out from growth cones of embryonic zebrafish, whereas we saw very little evidence of filopodia in the cat's optic nerve at any stage of development. Neither have filopodia been found in extensive three-dimensional reconstructions of growth cones in the optic nerve of primates (Williams and Rakic, '84, '85a).

Ultrastructure of growth cones. The axonal growth cone can be divided into two segments: a distal fringe, in our material made up almost exclusively of lamellipodia; and a core. This distinction is by no means original to our work; it can be traced back to early light microscopic studies of growth cones (Harrison, '10; Speidel, '33; Pomerant et al., '67), and has been described in detail in the *in vitro* ultrastructural studies of Yamada et al. ('70, '71) and Bunge ('73). In examination of several thousand growth cones *in situ* in this study it was clear from the outset that, as reported first reported by Tennyson ('70) and Yamada et al. ('70), the distal fringe of the growth cone contains little
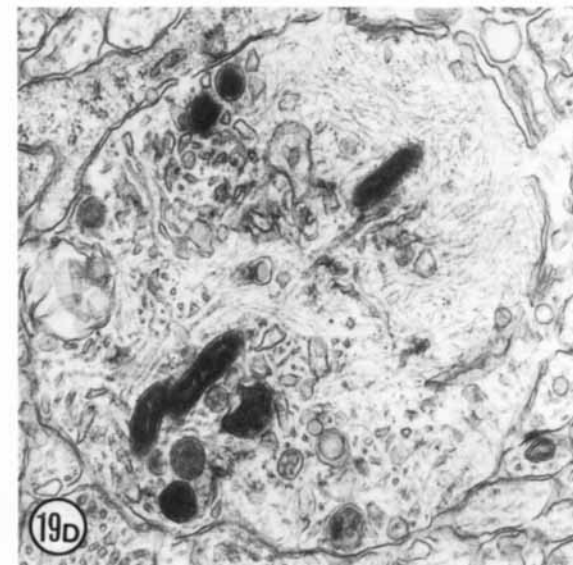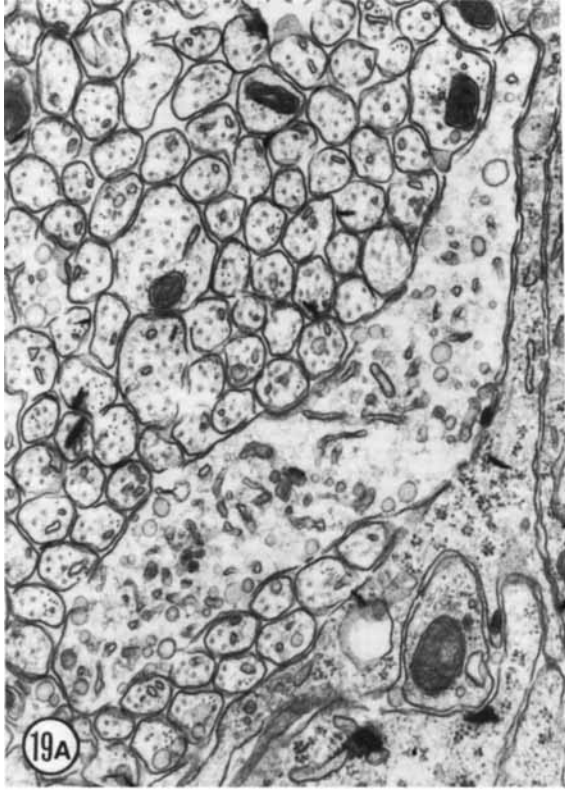
Fig. 19. Unusual, possibly necrotic growth cones at E-33. A. Large growth cone with an extraordinarily high vesicular content. ×25,000. B. The large inclusion and the accumulation of intermediate filaments in this neurite suggests that this process may be starting to die. ×25,000. C. Dilated growth cone with hyperplasia of neurofilaments and an accumulation of large dark-rimmed vesicles. ×26,000. D. Large fiber at an early stage of necrosis. The accumulation of neurofilaments in degenerating fibers is usually transitory and is followed by the condensation of the cytoplasm (cf., Lund, 1978, p. 45). ×26,000.
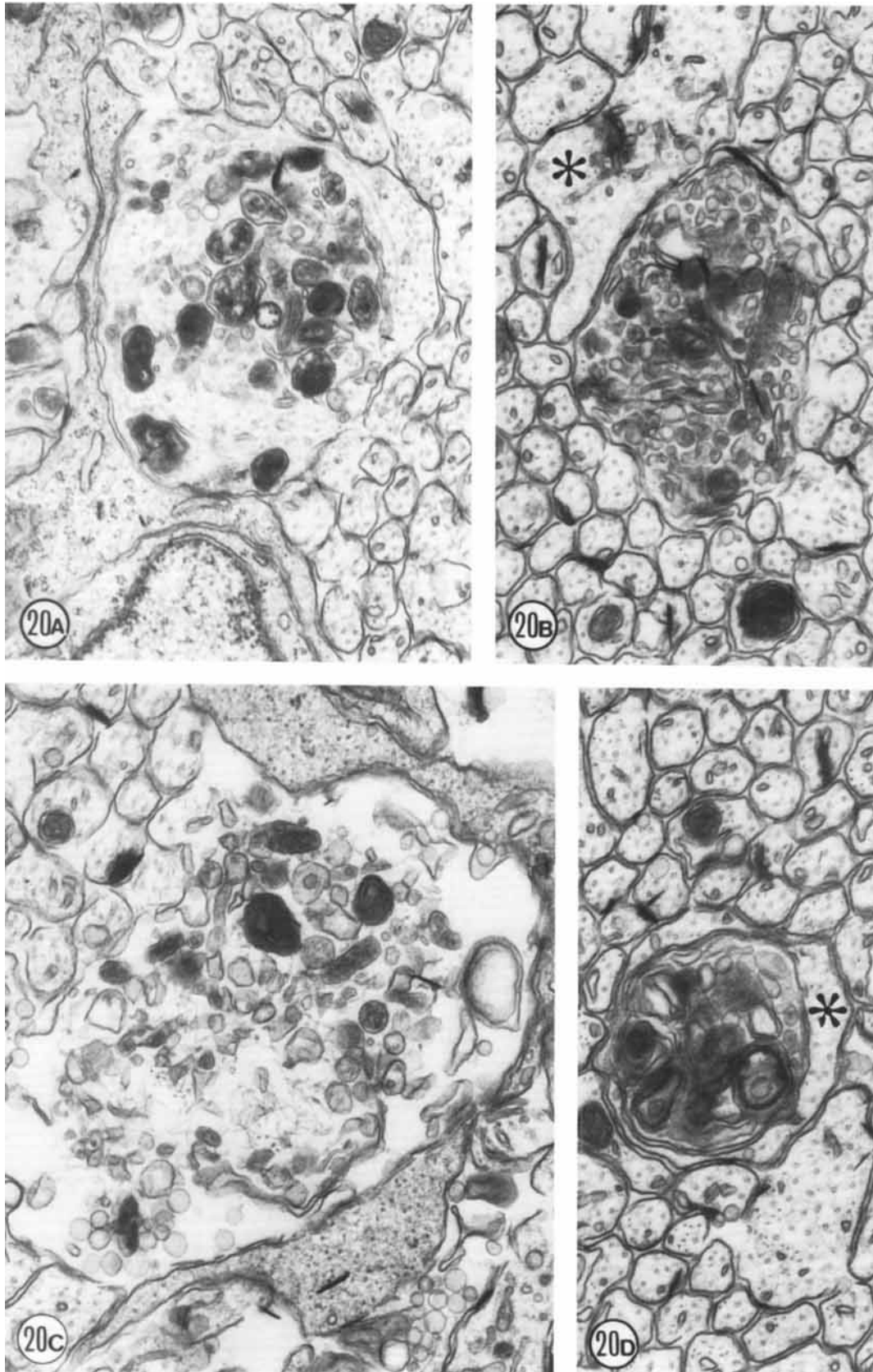
Fig. 20. Large necrotic fibers at E-33. A. An early stage of organelle accumulation and lysosome formation. ×26,000. B. Large fiber with condensed, vesicular cytoplasm. Note neighboring growth cone (asterisk) above necrotic fiber. ×34,000. C. Ruptured fiber. ×34,000. D. Highly condensed axoplasm that is either enveloped by or actually within a large and apparently normal fiber (asterisk). ×34,000.
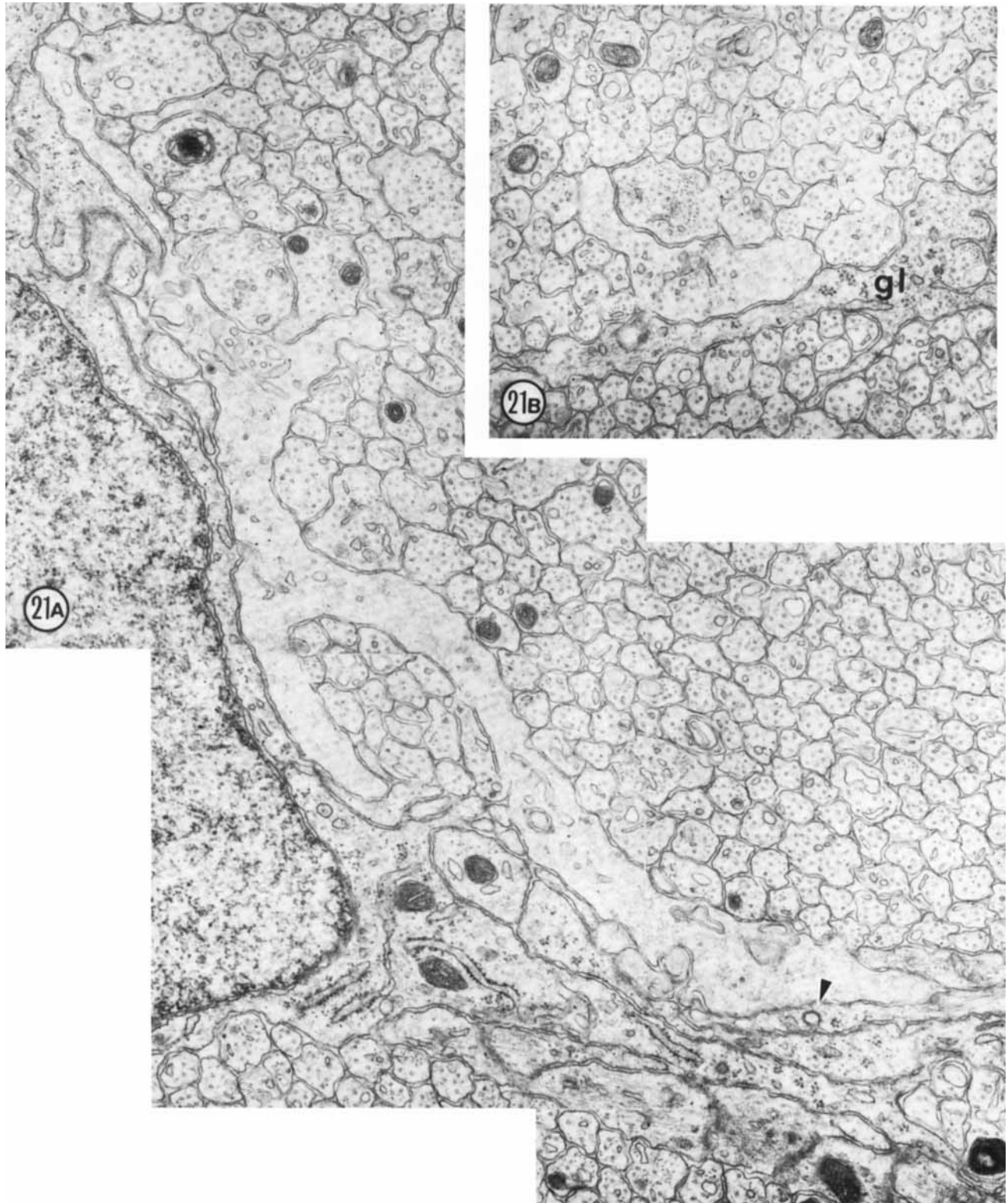
Fig. 21. A. One of the largest and last growth cones encountered in this study at E-39. This growth cone, located within 2 μm of the edge of the nerve, has a perimeter of about 25 μm and has 42 neighbors in this section. The density of all cytoplasmic components, even microfilaments, is low. Several types of vesicles, including a single dark-core vesicle, are present in the growth cone. A large coated pit forming within an astrocyte is marked with an arrowhead. ×25,000. B. Growth cone from a central fascicle. The ultrastructure of central and peripheral growth cones did not differ significantly, and although there is a marked difference in size between these two growth cones, this difference could easily have resulted from the level of section gl: glial process containing polyribosomes. ×38,000.
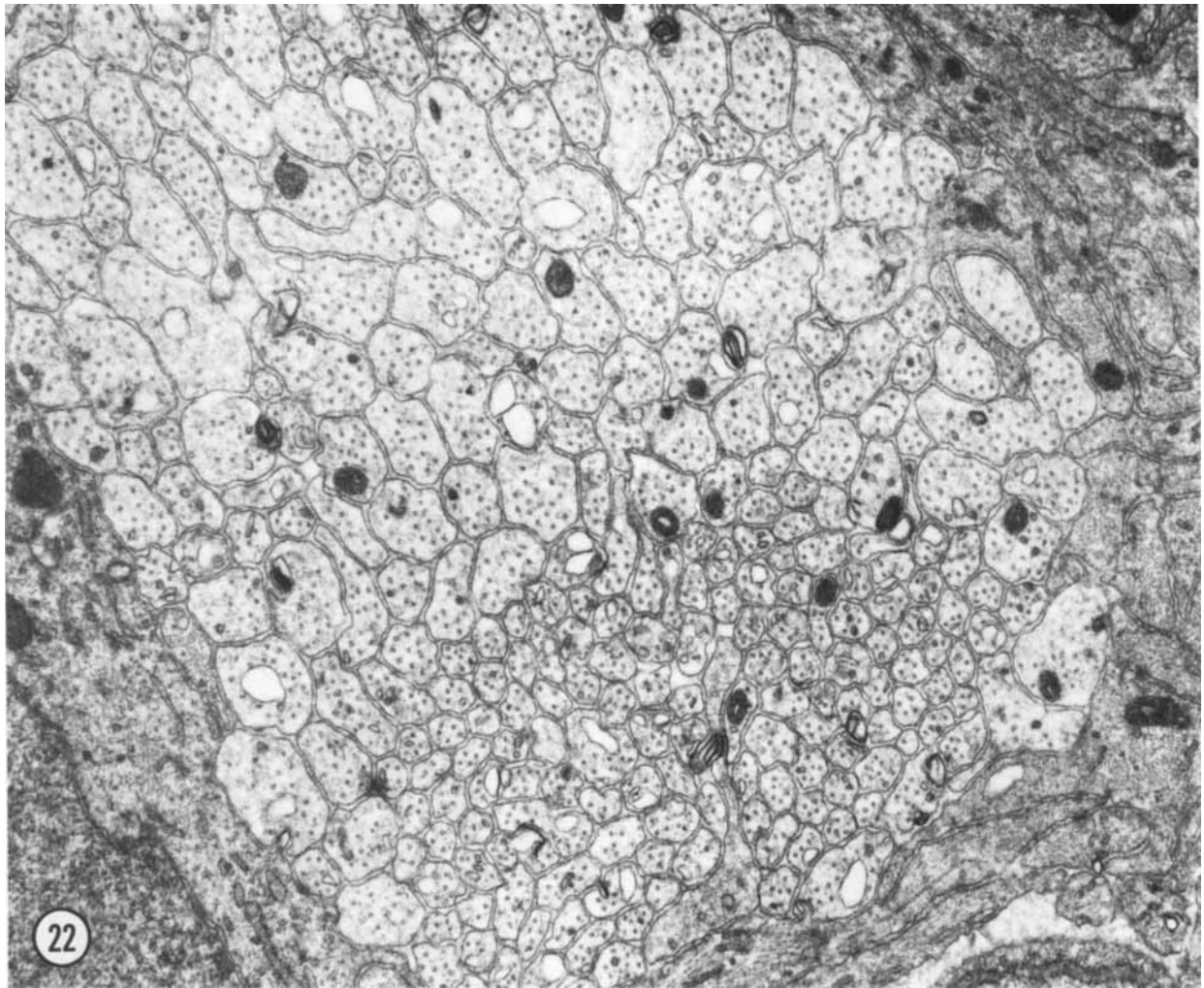
Fig. 22. E-44 optic nerve close to the periphery. The fibers in this fascicle appear to fall into two size groupings. Large axons in the upper half may either represent newly ingrown fibers that are sectioned close to their expanded tips or may simply represent a class of large axons. ×25,000.

more than a mesh of microfilaments that are closely associated with the inner wall of the plasma membrane and scattered clear vesicles. In contrast, the more proximal core, which Williams and Rakic ('84) have shown is located about 12 μm behind the leading edge, contains the cytoplasmic machinery of the growth cone. This is the site at which microtubules and neurofilaments terminate, and as a consequence it is also the site at which normal axoplasmic transport ends (reviewed in Lasek, '82). Here the axoplasm contains several classes of vesicles, mitochondria, and a complex network of tubes or sacks (see Cheng and Reese, '85) of what may be smooth endoplasmic reticulum (e.g., Figs. 10, 11).

As in the lamellipodia, large accumulations of clear, 40–120-nm vesicles were only rarely encountered in the core. Their scarcity surprised us because several previous studies have emphasized that aggregates of vesicles are a key feature of growth cones and that they are probably required to sustain rapid axon elongation (Bodian, '66a; Del Cerro and Snider, '68; Kawana et al., '71; Del Cerro, '74; Pfenninger and Bunge, '74). It should be noted, however, that only enough membrane needs to be added at the surface to

increase the length of a narrow-caliber axon by an amount equivalent to the forward movement of the growth cone; at a velocity of growth of 2 mm/day (more than twice the average velocity of a growth cone in the cat's optic nerve),[4] this amounts to 2,000 μm^2 of membrane for a typical axon with a diameter of 0.3 μm. The fusion of three 50-nm vesicles per second with the plasmalemma is sufficient to account for this growth. A large membrane reservoir is therefore probably not required, and those accumulations of vesicles that are occasionally encountered (e.g., Fig. 8) may be related to the retraction and internalization of lamellipodia, or may even be artifacts of glutaraldehyde

[4]We have shown that axons invade the optic stalk as early as E-19. The first complement of fibers approaches the dorsal lateral geniculate nucleus and the superior colliculus at about E-28 (Shatz and Kliot, '82; Shatz, '83). Since the distance between the posterior part of the eye and target nuclei in thalamus and midbrain is under 10 mm, the initial contingent of axons grow into the brain at an average velocity of between 0.5 and 1 mm per day.
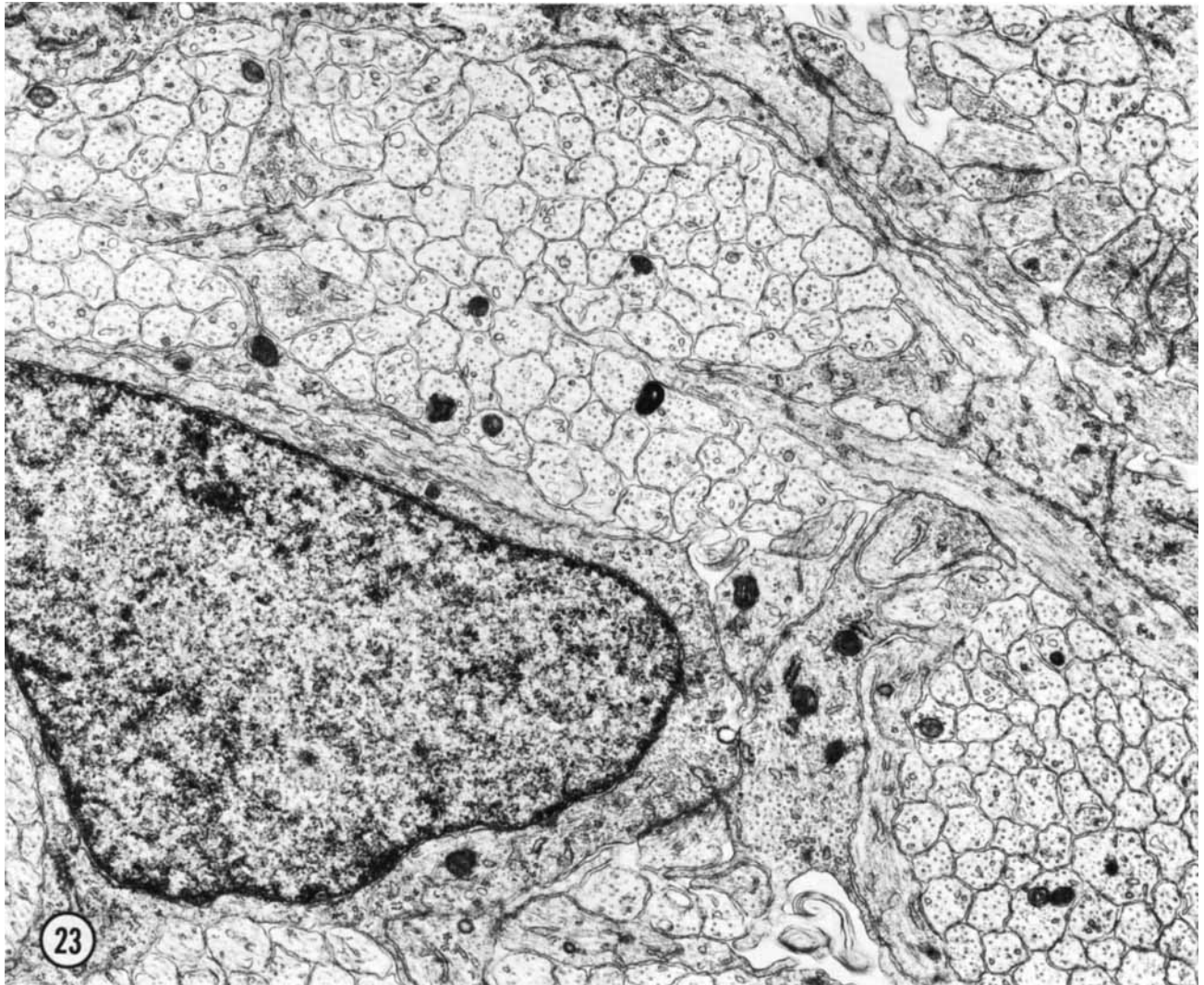
Fig. 23. E-53 optic nerve. Fascicles are subdivided repeatedly by astrocytic processes. Axons have much paler cytoplasm and far fewer intermediate filaments than do astrocytic fibers and astrocytic growth processes. ×15,600.

fixation (Hasty and Hay, '78; Nuttall and Wessells, '79; Falls and Gobel, '79; Chung and Reese, '85).

The shape of growth cones. There were age-related differences in the form and fine structure of growth cones. The differentiation between the distal fringe and the core was only rudimentary in the first growth cones that extended through the ducts of the optic stalk (Fig. 6); lamellipodia, when seen at all, were short and thick; microfilaments and neurofilaments were sparse. In contrast, growth cones that later grew within dense fascicles of axons in the optic nerve of older fetuses (E-28 and up) were with few exceptions characterized by large lamellipodia and organelle-rich core regions. This difference may have several causes: First, the simple shapes of the earliest growth cones may reflect the simple tubular environment of the optic stalk. Second, the comparatively low concentration of cytoskeletal components in these young growth cones may not be sufficient to support large lamellipodia. Third, the shape of growth cones may be influenced by the molecular composition of the surfaces along which they grow and by their

velocity of growth, and these factors may change with age (Agiro et al., '84). Finally, it is possible that all growth cones, irrespective of developmental stage, initially have simple morphology and that the pertinent distinction may actually be the age of individual growth cones—not that of the animal. Because ganglion cell generation proceeds from a region near the macula outward toward the retinal margin (Mall, 1893; Mann, '64; Walsh and Polley, '85), growth cones in nerves of older animals are invariably located at greater distances from the cell body than those in nerves of younger animals.

Distribution of growth cones. The tendency of fibers to add to the outer margins of the optic stalk and optic nerve was established in the last century by Müller (1874), Assheton (1892), and Robinson (1896). Assheton went so far as to state that fibers actually grew outside the stalk, like vines along a tree trunk. Robinson recognized correctly that fibers in fact pushed through spaces between the distal ends of neuroepithelial cells and were at all points actually within the central nervous system. In more recent studies,
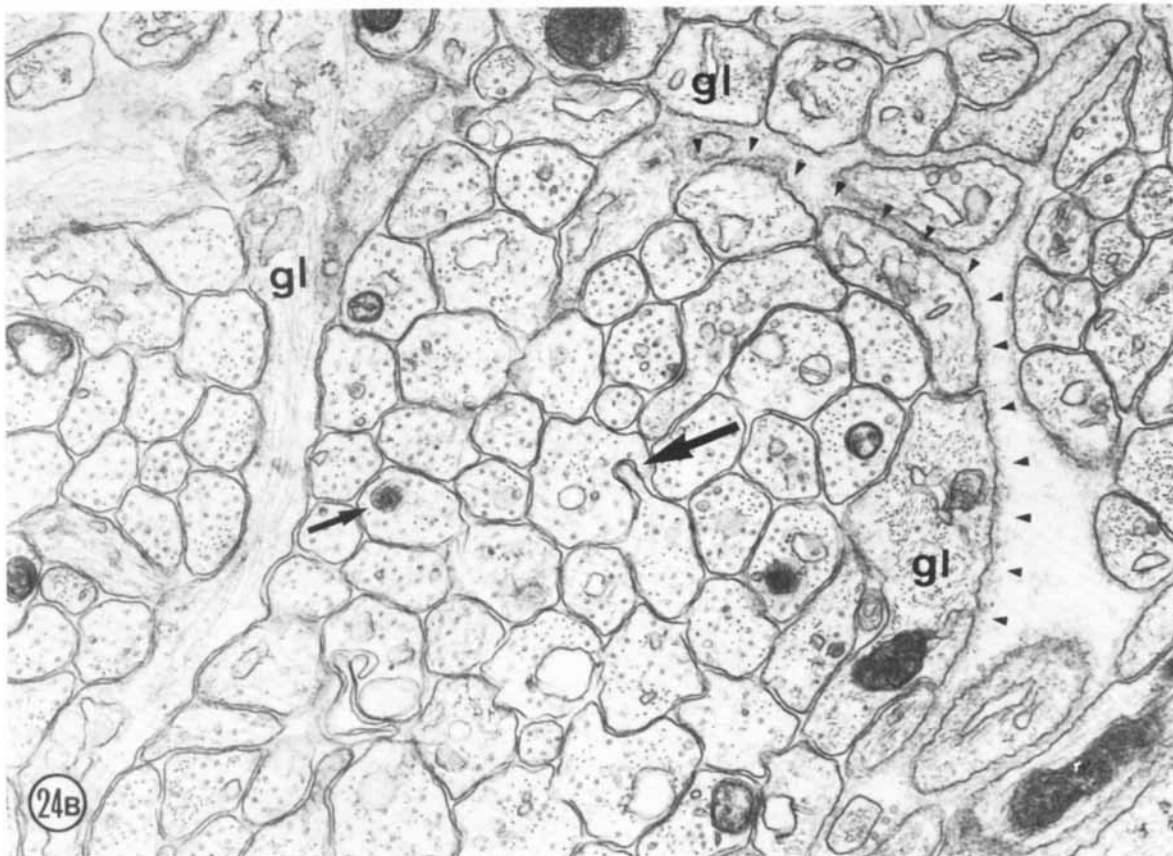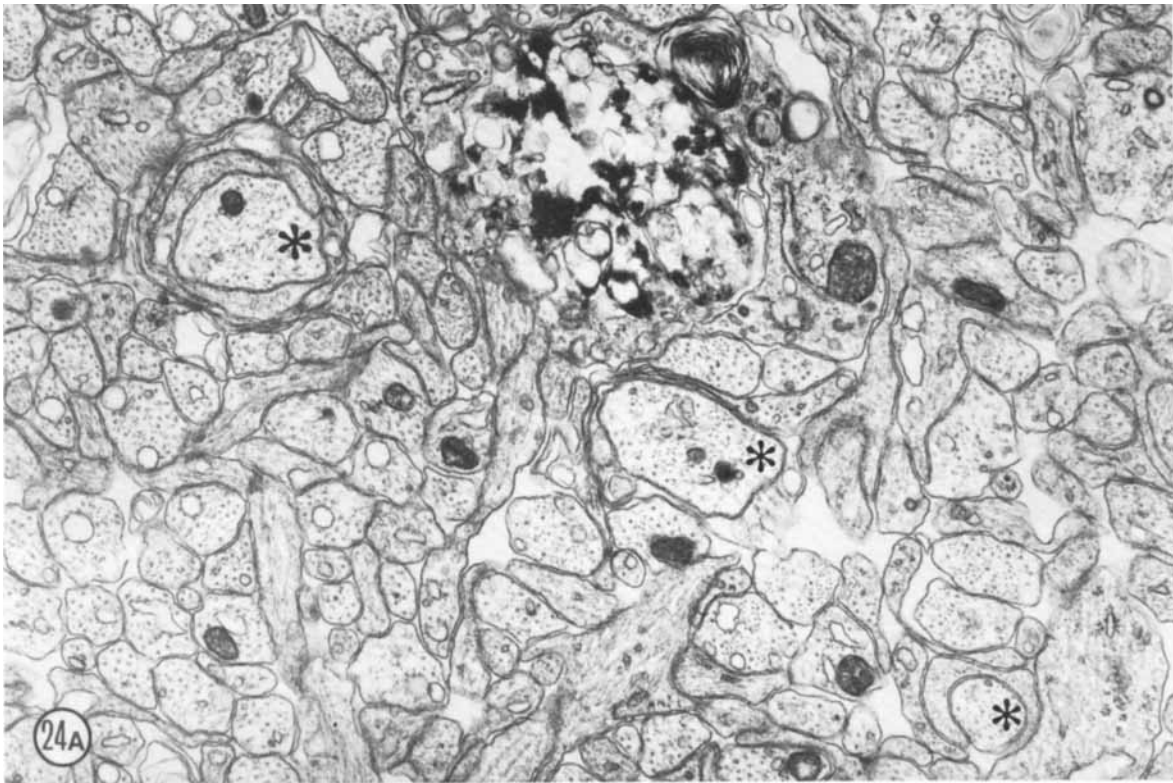
Fig. 24. Myelination at E-61. In A three axons marked by asterisks are in the process of being enveloped by glial tongues. Necrotic glial cells (dark, mottled region) and processes were common at this age and their presence may be related to the genesis of oligodendrocyte or the death of precursor cells. ×39,000. B. Axons and astrocytic processes at E-61 are hard often to distinguish from one another. Astrocyte fibers, a few of which are labeled (gl), generally have many intermediate filaments and less than three to four microtubules. Multivesicular body (small arrow) and axo-axonal invagination (large arrow). Basal lamina is marked with small arrowheads. ×64,000.
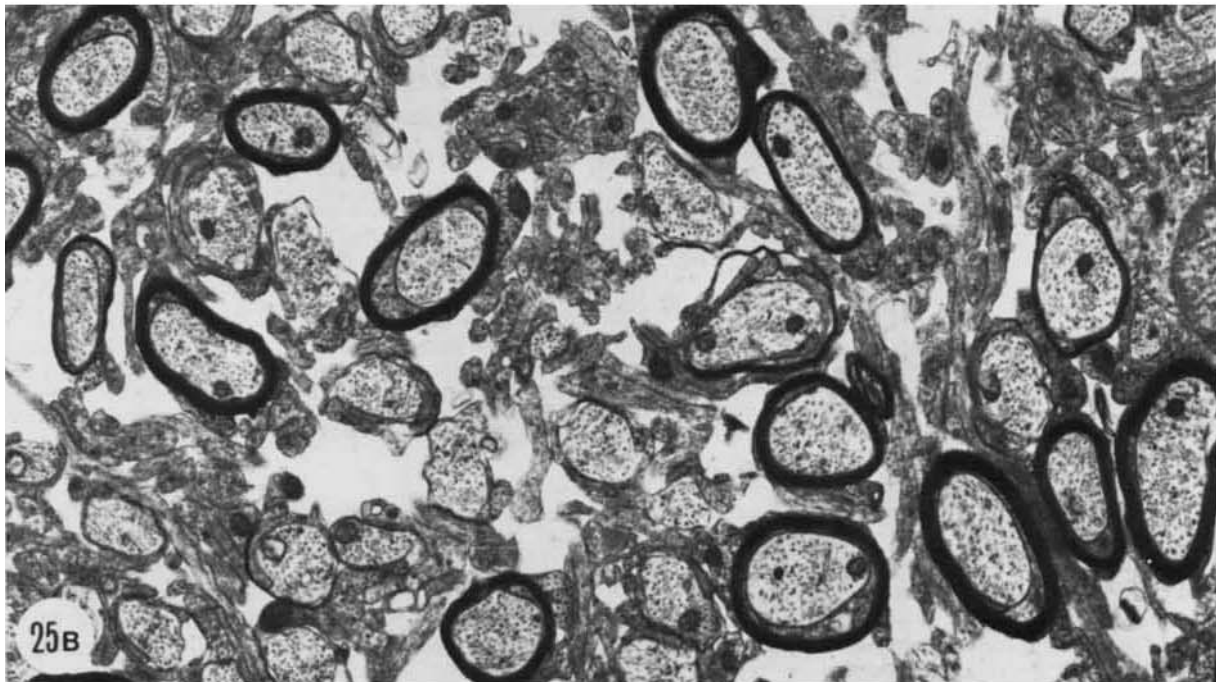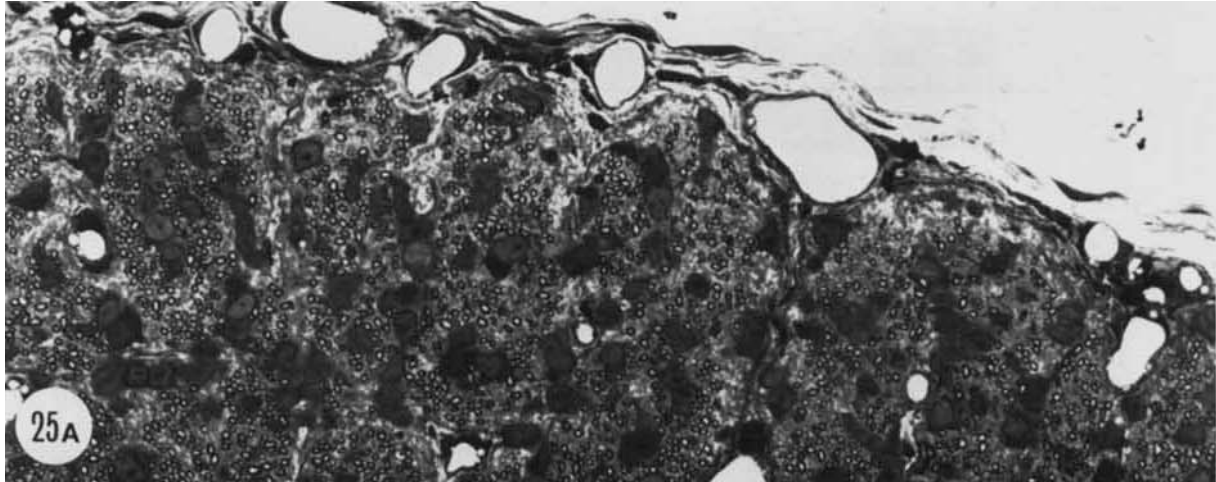
Fig. 25. Optic nerve at P-12—several days after eye opening. A. High-power light micrograph of the nerve during myelination. Large numbers of oligodendrocytes are intermixed with axons and as a consequence fascicular organization is disrupted. ×1,000. B. Fine structure of the nerve during myelination. The majority of axons in this field are either myelinated or are being enwrapped by glial processes. There is an increase in the amount of extracellular space during myelination. ×15,000. C,D. Necrotic myelinated axons (see page 54). ×25,000.

Fig. 26. Summary of the maturation of retinal ganglion cells and their projection to the dorsal lateral geniculate nucleus from the 20th day of gestation to 2 months after birth. The horizontal bars mark the approximate duration of events: black portions of these bars represent periods of peak intensity. References: 1. Walsh et al. ('83); 2. Hickey and Hitchcock ('84); 3. present study; 4. Shatz ('83); 5. Shatz ('83), Chalupa and Williams ('85); 6. Cragg ('75), Winfield et al. ('80), Mason ('82), Shatz and Kirkwood ('84); 7. Cragg ('75), Greiner ('80), Morrison ('77, '82); 8. Greiner ('80); 9. Moore et al. ('76) and this study; 10. Greiner ('80); 11. Sherman and Spear ('82); 12. Hubel and Wiesel ('70); 13. Mason ('82a,b), Sur et al. ('84).

it has been emphasized that growth cones of optic axons in a variety of species normally grow against the endfeet of neuroepithelial cells and near the extreme outer margins of the optic nerve (Silver and Sapiro, '81; Rager, '83; Silver and Rutishauser, '84). Although our results substantiate and amplify some of these observations, we stress that the central-to-peripheral gradient in growth cone distribution in the cat is actually quite modest at early stages of development: Growth cones are found in all fascicles, even those close to the center of the nerve. Even as late as E-39, when the gradient in the distribution of growth cones is comparatively steep, growth cones are still not uncommon in central parts of the optic nerve. Essentially the same pattern of fiber addition is also found in the optic nerve, chiasm, and tract of rhesus macaque fetuses (Williams and Rakic, '85b). In this species, growth cones are initially widely distributed in all parts of the pathway, but at later stages of development growth cones become progressively more restricted in their distribution and are eventually found only within 100 μm of the glial limiting membrane.

Necrotic fibers

Necrotic fibers occur commonly in central fiber tracts, peripheral nerves, and the gray matter at early stages of development (Bodian, '66b; Berger, '71a; Das and Hine, '72; Reier and Hughes, '71; Pannese, '76; Landmeser and Pilar, '76; Chu-Wang and Oppenheim, '78b; Cunningham et al., '82). There is substantial agreement that young unmyelin-

ated axons undergoing degeneration contain focal accumulations of autolytic debris, large vacuoles, and dense lamellar inclusions some of which are probably disintegrating mitochondria. As might be expected, these spontaneously degenerating axons have ultrastructural features often indistinguishable from unmyelinated axons in the mature nervous system undergoing experimentally induced Wallerian degeneration (e.g., Brooke et al., '65; Lampert, '67; Roth and Richardson, '69; Berger, '71b; Dyck and Hopkins, '72; Reier and Webster, '74; Bohn et al., '82; Williams et al., '85). Axons that we classified as necrotic in the optic nerve fit this description well (Figs. 17, 18). Degenerating axons in the nerve were surrounded by normal fibers and it is therefore not likely that they were artifacts of fixation or tissue processing. Furthermore, their incidence was greatest in the period during which the axon population was decreasing rapidly, and conversely very few such profiles were seen when the population was relatively stable.

The only previous study in which an attempt has been made to quantify the incidence of axon necrosis as a function of age is that of Landmesser and Pilar ('76). They demonstrated that during the peak of axon loss from the ciliary nerve of the chick embryo nearly 7–8% of all fibers were necrotic. Based upon their data it is possible to calculate a clearing time of axons of about 6–7 hours for axons. In contrast, we have estimated that it takes merely 1 hour to clear away the debris of an unmyelinated axon at a given

level along the optic nerve. Two assumptions underlie our estimate: First, the assumption that all axon loss is due to necrosis. If, however, a significant percentage of axons are retracted without autolysis of their constituents or disruption of membranes, then the clearing time of 1 hour will underestimate the true clearing time. Second, we have assumed that the duration of degradation of small, unmyelinated axons does not vary significantly with the time of day or fetal age. At present we have no reason to suspect that these are relevant variables, but if this proves incorrect then our estimate of clearing time will require adjustment. Furthermore, it is important to point out that our estimate of clearing time does not allow us to calculate the time required to eliminate the *entire* axon. If the process of axon elimination is analogous to burning a fuse, then we have simply determined the time required to burn a short piece of the fuse. The entire process of necrosis probably takes considerably longer than an hour. In fact, Rager ('80, p. 81) has estimated that the time constant for the degeneration of retinal ganglion cell axon in the chick is nearly 4 days.

It is unclear what removes axonal debris from the nerve. In other systems in which there is axon loss, glial cells or macrophages have been implicated in the phagocytosis of axonal debris. In the ventral roots, for instance, the rapid disintegration of more than half the axon population during embryogenesis is associated with the uptake of debris into Schwann cell phagosomes (Chu-Wang and Oppenheim, '78b) and similarly, during the early stages of Wallerian degeneration of the optic nerve, reactive astrocytes engulf large amounts of axon and myelin debris (Reier and Webster, '74). But we have been unable to find convincing signs of a similar process in the optic nerve during normal development, and in several instances it appeared that other optic fibers rather than astrocytes or macrophages had phagocytozed axon debris (Figs. 18G, 20D).

A number of very large necrotic fibers were noted in the optic nerve at the peak of axon ingrowth (Figs. 19, 20). None of these contained ribosomes, and because no similar processes were found in continuity with cell bodies we are confident that we have not misidentified the processes of glial cells. The large size of these necrotic fibers and their occurrence within fascicles of otherwise normal axons suggest that they may be the tips of dying fibers—the swollen terminal bulb described by Lampert ('67). Since these were not observed beyond E-39, after all growth cones had grown through the nerve, it is improbable that they were simply sections through dilated regions of normal-caliber axons in which debris had accumulated. We think it is likely that such structures as shown in Figures 19 and 20 are growth cones in the early stages of degeneration. Serial section analyses of such entities (R.W. Williams and P. Rakic, in progress) will allow us to verify this conclusion. As described by Speidel ('33), the first indications of impending death of a growing axon in the tadpole are the retraction of its lamellipodia and filopodia (he called them *sprouts*) and the balling up of the growth cone. Similarly, the retraction of growth cones *in vitro* is often associated with large accumulations of neurofilaments in discrete regions from which all other organelles are excluded (Yamada et al., '70, '71). This is precisely one of the most striking features of the growth cones reproduced in Figure 19. Such hyperplasia of neurofilaments is also seen commonly in terminals of retinal axons undergoing Wallerian degeneration (Guillery, '70; Lund, '78).

Magnitude of fiber loss and the estimate of total axon production. We have divided the loss of fibers in the cat's optic nerve into three phases. The first phase begins early in development, before E-28 and before axons have arborized extensively within their central targets. The number of axons lost during this period is not great— under 150,000. The second, more rapid phase of axon loss begins at a stage when the last growth cones are growing through the nerve and when target nuclei are being innervated. During this period, which lasts from about E-39 to E-53, as many as 500,000 axons are lost. The third phase of axon loss starts at about E-53 and extends until about P-36. During this long-lasting phase the rate of loss is very low, but even so, approximately 100,000 axons are eliminated. Although we can divide axon loss into three periods, we currently know disappointingly little about the causes that underlie the loss, and whether any given period is associated with a single dominant process.

Because the period of axon addition to the fetal cat's optic nerve overlaps that of axon loss for at least 11 days, many axons are eliminated even before the peak population is reached. As a consequence, to calculate the total production of axons it is necessary to determine how many fibers are lost before the peak and how many fibers are added after the peak. Although the need to provide for such a correction was recognized in at least one previous quantitative study of the developing optic nerve (Rakic and Riley, '83a), our work is the first in which an attempt has been made to provide the correction. On the basis of the time it takes to clear away axonal debris (approximately 1 hour), we estimated that 150,000 axons are lost before the peak is reached. In contrast, very few axons—probably fewer than 10,000 or 20,000—are added after the peak. Therefore, a total of about 800,000–900,000 axons are produced and grow into the optic nerve—five to six times the number in the adult nerve (Williams et al., '83, '85; Williams and Chalupa, '83b; Chalupa et al., '84).

Overlapping periods of axon generation and loss are common in many different parts of the nervous system. One of the most remarkable cases involves the development of the electric lobe (a cranial nerve nucleus) of the electric eel, in which neuron and axon production is vigorous during two periods of cell death (Fox and Richardson, '82, '84). Similarly, the overlap in the proliferation and death of neurons is so extensive in the spinal cord of *Xenopus* (Hughes, '61; Prestige, '65) and in the dorsal root ganglia of chick (Carr and Simpson, '82) that the total production of neurons is nearly twice as great as the peak population.

The time course and the magnitude of the developmental fluctuations in the fiber population of the cat that we have described in this paper differ in detail from the results of Ng and Stone ('82). They reported that there were 450,000–483,000 axons in the optic nerve from E-42 until as late as E-55. In contrast, we have shown that a peak of about 700,000 is reached by E-39 and that the fiber number decreases to the range of 200,000–300,000 as early as E-52. The discrepancies between their findings and the results reported here could conceivably reflect strain or sample variation. However, we think it is more likely that the method Ng and Stone used to estimate gestational age accounts for these differences. In their study several fetuses were removed by cesarean section from a litter of unknown age. The gestational age of these fetuses was then esti-

mated from the date the remainder of the litter was born, on the assumption that gestation was 65 days long. However, gestational age at birth is normally quite variable in the domestic cat (see Methods) and this variability is exacerbated by subjecting mothers to surgery during pregnancy. Based on our experience, such a method overestimates true gestational age by up to 6 days.

Rise and fall of axon number in relation to the development of retinal projections

One axon per retinal ganglion cell. What is the significance of the axon overproduction and axons loss, and how is the rise and fall in fiber number related quantitatively to changes in the ganglion cell population? We have recently shown that axons do not branch in the nerve at early stages of development (Lia et al., '86) and thus that the loss of axons in the fetal cat's optic nerve is not due to the elimination of axon collaterals. Nor is there evidence that ganglion cell axons branch to any significant degree before they reach the optic nerve in several other species. In a study of 340 embryonic chicken retinal wholemounts stained by the pyridine-silver technique, Goldberg and Coulumbre ('72) saw very few branched axons, and in these few cases the branches extended only 5–10 μm away from the cell body. Similarly, Hinds and Hinds ('74, '78) have shown that branching in the fiber layer of the embryonic mouse retina is extremely rare. Moreover, centrifugal and retino-retinal fibers (Bunt and Lund, '81) probably do not contribute significantly to the elevated fiber population in the optic nerve of the cat. The presence of centrifugal fibers can be ruled out almost entirely since labeled cells have not been seen after large intravitreal injections of horseradish peroxidase in numerous fetal cats (e.g., Williams and Chalupa, '82; Shatz, '83). While a retinoretinal projection appears to exist in the fetal cat, the number of cells involved is very small, well under 1% (B. Lia and L. M. Chalupa, unpublished; C. J. Shatz, personal communication). In sum, we feel justified in concluding that axons of ganglion cells do not branch, or branch only rarely, before the chiasm, and hence that there is close to a one-to-one correspondence between axons in the optic nerve and retinal ganglion cells in the cat at all stages of development.[5] Our conclusion is that nearly five out of six ganglion cells in the cat's retina are lost early in development.

Axon production and loss in relation to the genesis of retinal ganglion cells. Tritiated thymidine studies of ganglion cell neurogenesis in the cat have demonstrated that the first cells are generated in central retina before E-21 (Kliot and Shatz, '82; Walsh et al., '83; Walsh and Polley, '85) and that the last cells are generated after E-35. An analysis of the time-course of axon ingrowth into the nerve provides an independent means to assess the period of ganglion cell production. Our results demonstrate that ganglion cells are generated as early as E-19 and possibly as late as E-39. With the exception of the work of Kliot and Shatz ('82), these thymidine studies were based on the analysis of mature retinas, and the results therefore actually

apply only to that small fraction of ganglion cells that survive to maturity. In contrast, our admittedly less-direct method of assessing ganglion cell generation has the advantage of also taking into account those cells that ultimately die. The good correlation between these two very different methods implies that the population of cells that survive are generated within the same broad time period as those that are ultimately lost.

The central-to-peripheral distribution of growth cones we have described in the nerve could be a reflection of spatio-temporal gradients of ganglion cell generation (Walsh and Polley, '85). If correct, it follows that a degree of retinotopic order is retained within the developing optic nerve and that axons of neighboring ganglion cells grow along one another despite differences in time of generation. This seems unlikely, first because growth cones in the optic nerve do not track along preexisting fibers and consequently axons fail to retain neighbor relations (Williams and Rakic, '85), and second, because topographic order within the optic nerve is remarkably poor in adult cats (Horton et al., '79). At present we simply lack a good explanation for the gradient of growth cone density in the optic nerve.

Axon loss and target innervation. Ganglion cell axons first reach the posterior thalamus in detectable numbers by E-28 (Shatz, '83), at a stage when many neurons destined for the dorsal lateral geniculate nucleus are still migrating outward from the ventricular zone (Hickey and Hitchcock, '84). The ingrowth of optic axons into their target nuclei is at least roughly concurrent with the earliest age at which we have demonstrated dying fibers in the optic nerve (Fig. 26). A similar correlation between the onset of fiber loss and the arrival of fibers among target cells has also been found in several motor systems (Hughes, '65; Prestige, '67; Hamburger, '75; Landmesser and Morris, '75; Landmesser and Pilar, '76) and in the isthmo-optic projection of chick embryos (Clarke and Cowan, '76). Collectively, these observations support a hypothesis, most forcefully advanced by Hamburger and Oppenheim ('82), that those fibers that die do so because they are unable to compete effectively for trophic molecules released in target tissues. Two observations, however, make us doubt whether the earliest fiber loss is actually related to axon-target interactions. First, we found necrotic axon terminal bulbs in the optic nerve. Clearly, this observation, if correct, is difficult to reconcile with the idea that axon loss is related to interactions with target cells. Second, even as late as E-38, the density of fibers in the dorsal lateral geniculate nucleus and superior colliculus is low (Williams and Chalupa, '82; Shatz, '83; Chalupa and Williams, '85), extensive regions have only sparse input, and synaptic contacts of any sort are rare (Shatz and Kirkwood, '84). These observations are also difficult to reconcile with the idea that fiber loss is due solely to competitive interactions between axons for trophic molecules.

At the time the peak population of axons is reached (E-39), the retinal projection to the dorsal lateral geniculate nucleus, pretectum, and superior colliculus is still sparse. However, over the following week the density of the retinal influx becomes greater, and as early as E-47 virtually all parts of every retinorecipient nucleus contain a heavy input of retinal axons (Williams and Chalupa, '82, '83a; Shatz, '83; Chalupa and Williams, '84). Paradoxically, during this same period when the number of axons in the nerve drops by approximately 300,000, the density of innervation, as assessed by anterograde tracing methods, is on the rise.

---

[5]There is, of course, one caveat: During the peak of neurogenesis, the number of axons in the optic nerve will naturally lag behind the number of young ganglion cells since the most newly generated axons will not yet have grown through the nerve (Lia et al., '85).

Depending on one's bias, these results can be interpreted as showing either that fiber loss is unrelated to the formation of retinal connections or that the competition for trophic molecules during this period when terminal arbors are beginning to form is so fierce that many ganglion cells are unable to survive.

Axon loss and segregation. Segregation between axons from right and left eyes begins in the dorsal lateral geniculate nucleus at E-46 (Shatz, '83; Chalupa and Williams, '84, '85) and in the superior colliculus (Williams and Chalupa, '82) and pretectum (Williams and Chalupa, '83a) about a week later. Thus, the bulk of axons, some 400,000, are eliminated at least 1 week before the segregation of retinal projections is initiated. Indeed, the period when the most remarkable transformations in retinal projections are taking place corresponds to the slow phase of axon loss during which 50,000–150,000 fibers are lost. One of our principal reasons for examining fluctuations in the axon population was to determine to what degree axon loss could account for the formation of ocular dominance domains in the lateral geniculate nucleus and the superior colliculus. We conclude that while the loss of 50,000–150,000 axons could readily underlie the segregation of retinal projections, most fibers are eliminated for entirely different reasons (see the discussion of Chalupa and Williams, '85; and Sretavan and Shatz, '86). The relatively limited role of binocular competition in the loss of axons from the optic nerve of the cat is also demonstrated by the finding that the removal of one eye at a fetal age when the fiber population within the optic nerve is near its peak results in only a 20% increase in the number of fibers in the remaining optic nerve at maturity (Williams et al., '83; Chalupa et al., '84).

Axon loss and synpatogenesis. Besides segregation, two other major events occur during the last 2 weeks of gestation (Fig. 1B). First, the tempo of formation of retinal synapses increases greatly, and as early as eye opening the number of retinogeniculate synapses has been reported to be substantially greater than in the adult geniculate (Winfield et al., '80). Second, ganglion cell dendrites form synapses with amacrine and bipolar cells (Cragg, '75; Morrison, '77, '82; Greiner, '80). Although there are important gaps in our knowledge of the kinetics of synapse formation in the cat's visual system (and particularly the extent of turnover of early formed synapses), there is now enough evidence to conclude that approximately 100,000 retinal fibers are lost during the period when ganglion cells make the great majority of their synaptic contacts.

Axon loss and postnatal maturation of the visual system. The eyes of the kitten usually open during the early part of the second week, at about the same time that the first sluggish visual responses can be recorded from neurons in the superior colliculus (Stein et al., '73), dorsal lateral geniculate nucleus (Adrien and Roffwarg, '74; Daniels et al., '78; Beckmann and Albus, '82), and visual cortex (Hubel and Wiesel, '63; Albus and Wolf, '84). We have shown that even several days after eye opening (P-12), about 100,000 axons still remain to be eliminated, and this raises the possibility that the number of axons lost during this period may be affected by visual experience and ganglion cell activity. Our data and those of Z. Henderson (personal communication) demonstrate that the adult ganglion cell population is reached by the sixth week. Thus, the final population size is probably reached more than a month before the arbors of X- and Y-type retinal efferents have attained their characteristic dimensions (P-56 to P-90; see

Mason, '82a; and Sur et al., '84), several weeks before the segregation of ocular dominance columns in striate cortex is complete (ca. P-49; LeVay et al., '78), and probably just before the onset of the critical period (Hubel and Wiesel, '70; Sherman and Spear, '82).

Species comparisons

The overproduction of retinal ganglion cells and axons appears to be a fundamental characteristic of the development of the mammalian visual system. Overproduction of ganglion cells has also been reported in the only avian species examined to date, the chicken (Rager and Rager, '76; Rager, '80). A common denominator in the development of mammals and birds is that the proliferation of ganglion cells ends either before or shortly after birth. In contrast, in those cold-blooded vertebrates in which ganglion cells are generated throughout life (Straznicky and Gaze, '74) and in which the gradual increase in this population is accompanied by compensatory modifications of retinal connections (Gaze et al., '74; Scott and Lazar, '76; Easter and Stuermer, '84; Reh and Constantine-Paton, '84), there is no overproduction of optic fibers whatsoever (Gaze and Peters, '61; Wilson, '71; Easter et al., '81; Dunlop and Beazley, '84). Evidently, there are two strategies to arrive at suitable matches between the population of ganglion cells and the population of target cells. In mammals and birds a certain degree of flexibility during the formation of visual connections is achieved by producing more neurons than are ultimately needed (cf. Cowan, '73), whereas in two other classes—fish and amphia—the system is modifiable throughout life, thereby making the production of excess neurons or axons unnecessary.

However, it remains a puzzle why there should be such sizable differences in the degree of overproduction of ganglion cell axons in warm-blooded vertebrates. Why should there be a five- or sixfold overproduction in the domestic cat, a two- or threefold overproduction in primates (Rakic and Riley, '83a; van Driel and Provis, '83), and substantially less than a twofold overproduction in the chicken (Rager, '80)? Rakic ('85) has pointed out that those species with extensive fields of binocular vision and a greater uncrossed retinal projection—in particular, humans, rhesus monkeys, and cats—appear to lose a larger proportion of fibers and that the severity of axon loss may depend on the degree of intermingling and competition between axons from right and left eyes at early stages of development. In support of this idea, removal of one eye at early stages in different species (Rakic and Riley, '83b; Williams et al., '83; Chalupa et al., '84; Sefton and Lam, '84) reduces axon loss in the remaining optic nerve in proportion to the extent to which axons from right and left eye normally intermingle during development (Rakic, '85). However, it is clear that binocular competition does not explain the bulk of axon overproduction in most species, and, for instance, in the cat, the termination of binocular competition spares considerably less than one-tenth of those axons normally lost.

In a similar vein, it has been suggested that the loss of neurons and axons is a consequence of the elimination of topographically or functionally inappropriate connections (McLoon, '82; Jeffery and Perry, '82; Williams et al., '83; Insausti et al., '84; Jeffery, '84; Chalupa and Williams, '84; Jacobs et al., '84; O'Leary et al., '84; but see McLoon, '85). Although errors certainly do occur in small numbers during development, it seems unlikely that the degree of ganglion cell overproduction in different species is proportional to

the imprecision of connections. To be specific, it is unlikely that initial retinal connections in cat are so imprecise in comparison to other species that the most effective solution is to build in a five- or sixfold safety factor. In fact, recent results suggest that pattern of retinal projections, particularly the distribution of crossed and uncrossed fibers at the chiasm, are actually remarkably precise in fetal cats (Shatz and Kliot, '82; Lia et al., '83).

It is possible that differences in the magnitude of overproduction of ganglion cells and their axons have to do with recent evolutionary trends of different species (cf., Katz and Lasek, '78; Albrech et al., '79). During the late Pleistocene and particularly during the last 10 millenia, the body size of the species *Felis sylvestris*, of which the common cat is but a domestic variant *(Felis sylvestris catus)*, has become radically smaller (Kurtén, '65, '68; Hemmer, '74). As little as 15,000 years ago *Felis sylvestris* was more than twice as massive as either the domestic cat or most extant European and North African wildcats. Because brain size is proportional to body size—in nonprimate mammals the correlation (or allometric coefficient) between these variables is about 0.74 (Jerison, '73; Martin, '81; Eisenberg and Wilson, '82)—the recent reduction in the body size of the cat has probably been associated with a reduction in the size of the brain, eye, retina, and in total neuron number. Thus, some *fraction* of the ganglion cell excess in the fetal cat may be a phyletic holdover, and the elimination of this fraction may correspond to what Glücksmann ('51) refers to as phylogenetic cell death. In essence, we are arguing that the rapid reduction in the size of the cat has been achieved by changes in the developmental program that only take effect at comparatively late stages, well after ganglion cells have been generated. Although admittedly speculative, this idea can be tested: If correct, it follows that closely related, and much larger feline subspecies, particularly the Spanish wildcat, *Felis sylvestris tartessia*, should produce approximately the same number of retinal ganglion cells but fewer of these should be lost at later stages of development, and as a consequence the ganglion cell population at maturity should be greater than in the domestic cat.

Converging lines of evidence now indicate that multiple factors—among them axon-target interactions, competition for limited resources, and intrinsic programs of retinal development—regulate the severity of loss of retinal ganglion cells and their axons in mammals and birds. The substantial species differences provide important clues to the relative importance of these factors and may ultimately provide insight to the underlying utility of cell and fiber overproduction in brain development and evolution.

ACKNOWLEDGMENTS

LITERATURE CITED

Adrien, J., and H.P. Roffwarg (1974) Development of single-neuron responses in kitten's lateral geniculate nucleus. Exp. Neurol. 43:261–275.

Agiro, V., M.B. Bunge, and M.I. Johnson (1984) Correlation between growth (cone) form and movement and their dependence on neuronal age. J. Neurosci. 4:3051–3062.

Albrech, P., S.J. Gould, G.F. Oster, and D.B. Wake (1979) Size and shape in ontogeny and phylogeny. Paleobiology 5:296–317.

Albus, K., and W. Wolf (1984) Early post-natal development of neuronal function in the kitten's visual cortex: A laminar analysis. J. Physiol. (Lond.) 348:153–185.

Altman, J. (1971) Coated vesicles and synaptogenesis: A developmental study of the cerebellar cortex of the rat. Brain Res. 30:311–322.

Assheton, R. (1892) On the development of the optic nerve of vertebrates and the choroidal fissure of embryonic life. Q. J. Microsc. Sci. 34:85–104, plates 11, 12.

Bastiani, M.J., and C.S. Goodman (1984) Neuronal growth cones: Specific interactions mediated by filopodial insertion and induction of coated vesicles. Proc. Natl. Acad. Sci. U.S.A. 81:1849–1853.

Bastiani, M.J., J.A. Raper, and C.S. Goodman (1984) Pathfinding by neuronal growth cones in grasshopper embryos. III. Selective affinity of the G growth cone for the P cells within the A/P fascicle. J. Neurosci. 4:2311–2328.

Beckmann, R., and K. Albus (1982) The geniculocortical system in the early postnatal kitten: An electrophysiological investigation. Exp. Brain Res. 47:49–56.

Berger, B. (1971a) Quelques aspects ultrastructuraux de la substance blanche chez la souris Quaking. Brain Res. 25:35–53.

Berger, B. (1971b) Etude ultrastructurale de la dégénérescence Wallérienne experimentale d'un nerf entièrement amyélinique: Le nerf olfactif. I. Modifications axonales. J. Ultrastruct. Res. 37:105–118.

Black, M.M., and R.J. Lasek (1980) Slow component of axonal transport: Two cytoskeletal networks. J. Cell Biol. 86:616–623.

Bodian, D. (1966a) Development of fine structure of spinal cord in monkey foetuses. I. The motoneuron neuropil at the time of onset of reflex activity. Bull. Johns Hopkins Hosp. 119:129–149.

Bodian, D. (1966b) Spontaneous degeneration in the spinal cord of monkey foetuses. Bull. Johns Hopkins Hosp. 119:217–234.

Bodick, N. (1980) The Self-Assembly of the Embryonic Optic Nerve Into a Retinotopically Ordered Array. Ph.D. dissertation, Columbia University, New York. Ann Arbor, Michigan: University Microfilms International, Number 8104907.

Bohn, R.C., P.J. Reier, and E.B. Sourbeer (1982) Axonal interactions with connective tissue and glial substrata during optic nerve regeneration in Xenopus larvae and adults. Am. J. Anat. 165:397–419.

Brooke, R.N.L., de C. Downer, and T.P.S. Powell (1965) Centrifugal fibres to the retina in the monkey and cat. Nature 207:1365–1367.

Bunge, M.B. (1973) Fine structure of nerve fibers and growth cones of isolated sympathetic neurons in culture. J. Cell Biol. 56:713–735.

Bunt, S.M., and R.D. Lund (1981) Development of a transient retino-retinal pathway in hooded and albino rats. Brain Res. 211:399–404.

Carr, V.M., and S.B. Simpson (1982) Rapid appearance of labeled degenerating cells in the dorsal root ganglia after exposure of chick embryos to tritiated thymidine. Dev. Brain Res. 2:157–163.

Chalupa, L.M., and R.W. Williams (1984) Prenatal development and reorganization in the visual system of the cat. In J. Stone, B. Dreher, and D.H. Rapaport (eds): Development of Visual Pathways in Mammals. New York: Alan R. Liss, pp. 89–102.

Chalupa, L.M., and R.W. Williams (1985) Formation of retinal projections in the cat. In R.N. Aslin (ed): Advances in Neuronal and Behavioral Development. vol. 1. Norwood, New Jersey: Ablex Publishing, pp. 1–32.

Chalupa, L.M., R.W. Williams, and Z. Henderson (1984) Binocular interaction in the fetal cat regulates the size of the ganglion cell population. Neuroscience 12:1139–1146.

Cheng, T.P.O., and T.S. Reese (1985) Polarized compartmentalization of organelles in growth cones from developing optic tectum. J. Cell Biol. 101:1473–1480.

Chu-Wang, I.-W., and R.W. Oppenheim (1978a) Cell death of motoneurons in the chick embryo spinal cord. I. A light and electron microscopic study of naturally occurring and induced cell loss during development. J. Comp. Neurol. 177:33–58.

Chu-Wang, I.-W., and R.W. Oppenheim (1978b) Cell death of motoneurons in the chick embryo spinal cord. II. A quantitative and qualitative analysis of degeneration in the ventral root, including evidence for axon outgrowth and limb innervation prior to cell death. J. Comp. Neurol. 177:59–86.

Cima, C., and P. Grant (1980) Ontogeny of the retina and optic nerve of Xenopus laevis. IV. Ultrastructural evidence of early ganglion cell differentiation. Dev. Biol. 76:229–237.

Cima, C., and P. Grant (1982) Development of the optic nerve in Xenopus laevis. I. Early development and organization. J. Embryol. Exp. Morphol. 72:225–249.

Clarke, P.G.H., amd W.M. Cowan (1976) The development of the isthmo-optic tract in the chick, with special reference to the occurrence and correction of developmental errors in the location and connection of isthmo-optic neurons. J. Comp. Neurol. 167:143–164.

Cochran, W.G. (1963) Sampling Technique (2nd ed). New York: John Wiley & Sons.

Cook, R.D. and H.M. Wiśniewski (1973) The role of oligodendroglia and astroglia in Wallerian degeneration of the optic nerve. Brain Res. 61:191–206.

Cook, R.D., B.D. Ghetti, and H.M. Wiśniewski (1974) The pattern of Wallerian degeneration in the optic nerve of the newborn kitten: An ultrastructural study. Brain Res. 75:261-275.

Cowan, W.M. (1973) Neuronal death as a regulative mechanism in the control of cell number in the nervous system. In M. Rockstein (ed): Development and Aging in the Nervous System. New York: Academic Press, pp. 19-41.

Cragg, B.G. (1975) The development of synapses in the visual system of the cat. J. Comp. Neurol. 160:147-166.

Crespo, D., D.D.M. O'Leary, and W.M. Cowan (1985) Changes in the numbers of optic nerve fibers during late prenatal and postnatal development in the albino rat. Dev. Brain Res. 19:129-134.

Cunningham, T.J., I.M. Mohler, and D.L. Giordano (1982) Naturally occurring neuron death in the ganglion cell layer of the neonatal rat: Morphology and evidence for regional correspondence with neuron death in superior colliculus. Dev. Brain Res. 2:203-215.

Daniels, J.D., J.D. Pettigrew, and J.L. Norman (1978) Development of single-neuron responses in kitten's lateral geniculate nucleus. J. Neurophysiol. 41:1373-1393.

Das, G.D., and R.J. Hine (1972) Nature and significance of spontaneous degeneration of axons in the pyramidal tract. Z. Anat. Entwickl.-Gesch. 136:98-114.

Del Cerro, M.P. (1974) Uptake of tracer proteins in the developing cerebellum, particularly by the growth cones and blood vessels. J. Comp. Neurol. 157:245-280.

Del Cerro, M.P., and R.S. Snider (1968) Studies on the developing cerebellum. Ultrastructure of the growth cones. J. Comp. Neurol. 133:341-362.

Donovan, A. (1966) The postnatal development of the cat retina. Exp. Eye Res. 5:249-254.

Droz, B. (1963) Axonal migration of proteins in the central nervous system and peripheral nerves as shown by radioautography. J. Comp. Neurol. 121:325-346.

Dunlop, S.A., and L.D. Beazley (1984) A morphometric study of the retinal ganglion layer and optic nerve from metamorphosis in Xenopus. Vis. Res. 24:417-427.

Dyck, P.J., and A.P. Hopkins (1972) Electron microscopic observations on degeneration and regeneration of unmyelinated fibres. Brain 95:223-234.

Easter, S.S., Jr., A.C. Rusoff, and P.E. Kish (1981) The growth and organization of the optic nerve and tract in juvenile and adult goldfish. J. Neurosci. 1:793-811.

Easter, S.S., Jr., and C.A.O. Stuermer (1984) An evaluation of the hypothesis of shifting terminals in goldfish optic tectum. J. Neurosci. 4:1052-1063.

Easter, S.S., Jr., B. Bratton, and S.S. Scherer (1984) Growth-related order of the retinal fiber layer in goldfish. J. Neurosci. 4:2173-2190.

Eisenberg, J.F., and D.E. Wilson (1982) Relative brain size and feeding strategies in the Chiroptera. Evolution 32:740-751.

Falls, W., and S. Gobel (1979) Golgi and EM studies of the formation of dendritic and axonal arbors: The interneurons of the substantia gelatinosa of Rolando in newborn kittens. J. Comp. Neurol. 187:1-18.

Fox, G.Q., and G.P. Richardson (1982) The developmental morphology of Torpedo marmorata: Electric lobe-electromotoneuron proliferation and cell death. J. Comp. Neurol. 207:183-190.

Fox, G.Q., and G.P. Richardson (1984) Neuronal cell death in the electric lobe of Torpedo marmorata. Soc. Neurosci. Abst. 10:641.

Gaze, R.M., and A. Peters (1961) The development, structure and composition of the optic nerve of Xenopus laevis (Daudin). Q. J. Exp. Physiol. 46:299-309.

Gaze, R.M., M.J. Keating, and S.H. Chung (1974) The evolution of the retinotectal map during development in Xenopus. Proc. R. Soc. Lond. [Biol.] 185:301-330.

Glücksmann, A. (1951) Cell deaths in normal vertebrate ontogeny. Biol. Rev. 26:59-89.

Goldberg, S., and A.J. Coulombre (1972) Topographical development of the ganglion cell fiber layer in the chick retina. A whole mount study. J. Comp. Neurol. 146:507-518.

Grafstein, B., and M. Murray (1969) Transport of protein in goldfish optic nerve during regeneration. Exp. Neurol. 25:494-508.

Greiner, J.V., and T.A. Weidman (1980) Histogenesis of the cat retina. Exp. Eye Res. 30:439-453.

Greulich, W.W. (1934) Artificially induced ovulation in the cat (Felis domestica). Anat. Rec. 58:217-224.

Guillery, R.W. (1970) Light- and electron-microscopical studies of normal and degenerating axons. In W.J.H. Nauta and S.O.E. Ebbesson (eds): Comtemporary Research Methods in Neuroanatomy. New York: Springer-Verlag, pp. 77-105.

Gundersen, H.J.G. (1977) Notes on the elimination of the numerical density of arbitrary profiles: The edge effect. J. Microsc. 111:219-223.

Halfter, W., and S. Deiss (1984) Axon growth in embryonic chick and quail retinal whole mounts in vitro. Dev. Biol. 102:344-355.

Hamburger, V. (1975) Cell death in the development of the lateral motor column of the chick embryo. J. Comp. Neurol. 160:535-546.

Hamburger, V., and R.W. Oppenheim (1982) Naturally occurring neuronal death in vertebrates. Neurosci. Comm. 1:39-55.

Harrison, R.G. (1910) The outgrowth of the nerve fiber as a mode of protoplasmic movement. J. Exp. Zoöl. 17:521-544.

Hasty, D.L., and E.D. Hay (1978) Freeze-fracture studies of the developing cell surface. II. Particle-free membrane blisters in glutaraldehyde fixed corneal fibroblasts are artifacts. J. Cell Biol. 78:756-768.

Hemmer, H. (1974) Fossil History of Living Felidae. In R.L. Eaton (ed): The World's Cats. vol. 3, no. 2. Contributions to Biology, Ecology, Behavior and Evolution. Seattle: Carnivore Research Institute, Burke Museum, University of Washington, pp. 58-61.

Hendrickson, A., and W.M. Cowan (1971) Changes in the rate of axoplasmic transport during postnatal development of the rabbit's optic nerve and tract. Exp. Neurol. 30:403-422.

Herron, M.A., and R.F. Sis (1974) Ovum transport in the cat: Effects of estrogen administration. Am J. Vet. Res. 35:1277-1279.

Hickey, T.L., and P.F. Hitchcock (1984) Genesis of neurons in the dorsal lateral geniculate nucleus of the cat. J. Comp. Neurol. 228:186-199.

Hildebrand, C. (1971) Ultrastructural and light-microscopic studies of the developing feline spinal cord white matter. II. Cell death and myelin sheath disintegration in the early postnatal period. Acta Physio. Scand. [Suppl.] 364:109-114.

Hinds, J.W., and P.L. Hinds (1974) Early ganglion cell differentiation in the mouse retina: An electron microscopic analysis utilizing serial sections. Dev. Biol. 37:381-416.

Hinds, J.W., and P.L. Hinds (1978) Early development of amacrine cells in the mouse retina: An electron microscopic, serial section analysis. J. Comp. Neurol. 179:277-300.

Hoogeweg, J.H., and E.R. Folkers, Jr. (1970) Superfetation in a cat. J. Am. Vet. Med. Assoc. 156:73-75.

Horton, J.C., M.M. Greenwood, and D.H. Hubel (1979) Non-retinotopic arrangement of fibres in cat optic nerve. Nature 282:720-722.

Hubel, D.H., and T.N. Wiesel (1963) Receptive fields of cells in striate cortex of very young, visually inexperienced kittens. J. Neurophysiol. 26:994-1002.

Hubel, D.H., and T.N. Wiesel (1970) The period of susceptibility to the physiological effects of unilateral eye closure in kittens. J. Physiol. (Lond.) 206:419-436.

Hughes, A.F. (1961) Cell degeneration in the larval ventral horn of Xenopus laevis. J. Embryol. Exp. Morphol. 9:269-284.

Hughes, A.F. (1965) A quantitative study of the development of the nerves in the hind-limb of Eleutherodactylus martinicensis. J. Embryol. Exp. Morphol. 13:9-34.

Illing, R.-B., and H. Wässle (1981) The retinal projection to the thalamus in the cat: A quantitative investigation and a comparison with the retinotectal pathway. J. Comp. Neurol. 202:265-285.

Insausti, R., C. Blakemore, W.M. Cowan (1984) Ganglion cell death during development of ipsilateral retino-collicular projections in golden hamster. Nature 308:362-365.

Jacobs, D.S., V.H. Perry, and M.J. Hawken (1984) The postnatal reduction of the uncrossed projection from the nasal retina in the cat. J. Neurosci. 4:2425-2433.

Jeffery, G. (1984) Retinal ganglion cell death and terminal field retraction in the developing rodent visual system. Dev. Brain Res. 13:81-96.

Jeffery, G., and V.H. Perry (1982) Evidence for ganglion cell death during development of the ipsilateral retinal projection in the rat. Dev. Brain Res. 2:176-180.

Jerison, H.J. (1973) Evolution of the Brain and Intelligence. New York: Academic Press.

Katz, M.J., and R.J. Lasek (1978) Evolution of the nervous system: Role of ontogenetic mechanisms in the evolution of matching populations. Proc. Natl. Acad. Sci. U.S.A. 75:1349-1352.

Kawana, E., C. Sandri, and K. Akert (1971) Ultrastructure of growth cones in the cerebellar cortex of the neonatal rat and cat. Z. Zellforsch. 155:284-298.

Kirby, M.A., and P.D. Wilson (1984) Axon count in the developing optic nerve of the North American opossum: Overproduction and elimination. Soc. Neurosci. Abst. 10:467.

Kliot, M., amd C.J. Shatz (1982) Genesis of different retinal ganglion cell types in the cat. Soc. Neurosci. Abst. 8:815.

Krayanek, S., and S. Goldberg (1981) Oriented extracellular channels and axonal guidance in the embryonic chick retina. Dev. Biol. *84:*41–50.

Kurtén, B. (1965) On the evolution of the European wild cat, *Felis silvestris* Schreber. Acta Zool. Fenn. *111:*1–29.

Kurtén, B. (1968)Pleistocene Mammals of Europe. Chicago: Aldine Publishing Co.

Lampert, P.W. (1967) A comparative electron microscopic study of reactive, degenerating, regenerating, and dystrophic axons. J. Neuropathol. Exp. Neurol. *26:*345–368.

Landmesser, L., and D.G. Morris (1975) The development of functional innervation in the hind-limb of the chick embryo. J. Physiol. (Lond.) *249:*301–326.

Landmesser, L., and G. Pilar (1976) Fate of ganglionic synapses and ganglion cell axons during normal and induced cell death. J. Cell Biol. *68:*357–374.

Lasek, R.J. (1982) Translocation of the neuronal cytoskeleton and axonal locomotion. Philos. Trans. R. Soc. Lond. Biol. *299:*313–327.

LeVay, S., M.P. Stryker, and C.J. Shatz (1978) Ocular dominance columns and their development in layer IV of the cat's visual cortex: A quantitative study. J. Comp. Neurol. *191:*223–244.

Lia, B., R.W. Williams, and L.M. Chalupa (1983) Early development of retinal specialization: The distribution and decussation patterns of ganglion cells in the prenatal cat demonstrated by retrograde peroxidase labeling. Soc. Neurosci. Abst. *9:*702.

Lia, B., R.W. Williams, and L.M. Chalupa (1986) Does axonal branching contribute to the overproduction of optic nerve fibers during early development of the cat's visual system? Dev. Brain Res. (in press).

Lund, R.D. (1978) Development and Plasticity of the Brain. New York: Oxford Univ. Press.

Mall, F. (1893) Histogenesis of the retina in ambystoma and necturus. J. Morphol. *8:*415–432.

Mann, I. (1964) The Development of the Human Eye (3rd ed). London: British Medical Association.

Marin-Padilla, M. (1971) Early prenatal ontogenesis of the cerebral cortex (neocortex) of the cat *(Felis domestica).* A Golgi study. Z. Anat. Entwickl.-Gesch. *134:*117–145.

Martin, P. (1891) Zur Entwickelung der Netzhaut bei der Katze. Zeit. f. vergleich. Augenheilkunde *7:*25–41.

Martin, R.D. (1981) Relative brain size and basal metabolic rate. Nature *293:*57–60.

Mason, C.A. (1982a) Development of terminal arbors of retino-geniculate axons in the kitten—I. Light microscopical observations. Neuroscience *7:*541–559.

Mason, C.A. (1982b) Development of terminal arbors of retino-geniculate axons in the kitten—II. Electron microscopical observations. Neuroscience *7:*561–582.

Mastronarde, D.M., M.A. Thibeault, and M.W. Dubin (1984) Non-uniform postnatal growth of the cat retina. J. Comp. Neurol. *228:*598–608.

McLoon, S.C. (1982) Alteration in precision of the crossed retinotectal projection during chick development. Science *215:*1418–1420.

McLoon, S.C. (1985) Elimination of the transient ipsilateral retinotectal projection in the developing chick. Soc. Neurosci. Abs. *11:*222.

Moore, C.L., R. Kalil, and W. Richards (1976) Development of myelination in optic tract of the cat. J. Comp. Neurol. *165:*125–136.

Mori, S., amd C.P. LeBlond (1970) Electron microscopic identification of three classes of oligodendrocytes and a preliminary study of their proliferative activity in the corpus callosum of young rats. J. Comp. Neurol. *139:*1–30.

Morrison, J.D. (1977) Electron microscopic studies of developing kitten retina. J. Physiol. (Lond.) *273:*91p–92p.

Morrison, J.D. (1982) Postnatal development of the area centralis of the kitten retina: An electron microscopic study. J. Anat. *135:*255–271.

Müller, W. (1874) Ueber die Stammesentwicklung des Sehorgans der Wirbelthiere. Beitraege z. Anat. u. Physiol. als Festgabe Carl Ludwig, vol.2, Leipzig: Verlag von F.C.W. Vogel, pp. 1–76, plates 10–14.

Nabeshima, S., T.S. Reese, D.M.D. Landis, and M.W. Brightman (1975) Junctions in the meninges and marginal glia. J. Comp. Neurol. *164:*127–170.

Nathaniel, E.J.H., and D.C. Pease (1963) Degenerative changes in rat dorsal roots during Wallerian degeneration. J. Ultrastruct. Res. *9:*511–532.

Ng, A.Y.K., and J. Stone (1982) The optic nerve of the cat: Appearance and loss of axons during normal development. Dev. Brain Res. *5:*263–271.

Nuttall, R.P., and N.K. Wessells (1979) Veils, mounds, and vesicle aggregates in neurons elongating in vitro. Exp. Cell Res. *119:*163–174.

O'Leary, D.D.M., J.W. Fawcett, and W.M. Cowan (1984) Elimination of topographical targeting errors in the retinocollicular projection by ganglion cell death. Soc. Neurosci. Abstr. *10:*464.

Pachter, J.S., and R.K.H. Liem (1984) The differential appearance of neurofilament triplet polypeptides in the developing rat optic nerve. Dev. Biol. *103:*200–210.

Pannese, E. (1976) An electron microscopic study of degeneration in chick embryo spinal ganglia. Neuropathol. Appl. Neurobiol. *2:*247–267.

Perry, V.H., Z. Henderson, and R. Linden (1983) Postnatal changes in retinal ganglion cell and optic axon populations in the pigmented rat. J. Comp. Neurol. *219:*356–368.

Peters, A., and J.E. Vaughn (1967) Microtubules and filaments in the axons and astrocytes of early postnatal rat optic nerves. J. Cell Biol. *32:*113–119.

Pfenninger, K.H., and R.P. Bunge (1974) Freeze-fracturing of nerve growth cones and young fibers. A study of the developing plasma membrane. J. Cell Biol. *63:*180–196.

Polley, E.H., C. Walsh, and T.L. Hickey (1981) Neurogenesis in the inner nuclear layer (INL) and outer nuclear layer (ONL) of the cat retina: A study using ^{3}H-thymidine. Invest. Ophthalmol. Vis. Sci. [Suppl.] *22:*114.

Pomerat, C.M., W.J. Hendelman, C.W. Raiborn, Jr., and J.F. Massey (1967) Dynamic activities of nervous tissue *in vitro.* In H. Hydén (ed): The Neuron. New York: Elsevier Publishing Co., pp. 119–178.

Prescott, C.W. (1973) Reproduction patterns in the domestic cat. Austral. Vet. J. *49:*126–134.

Prestige, M.C. (1965) Cell turnover in the spinal ganglia of *Xenopus laevis* tadpoles. J. Embryol. Exp. Morphol. *13:*63–72.

Prestige, M.C. (1967) The control of cell number in the lumbar ventral horns during the development of *Xenopus laevis* tadpoles. J. Embryol. Exp. Morphol. *18:*359–387.

Provis, J.M., D. van Driel, F.A. Billson, and P. Russell (1985) Human fetal optic nerve: Overproduction and elimination of retinal axons during development. J. Comp. Neurol. *238:*92–101.

Rager, G. (1980) Development of the retinotectal projection in the chicken. Adv. Anat. Embryol. Cell Biol. *63:*1–92.

Rager, G. (1983) Structural analysis of fiber organization during development. In J.-P. Changeux, J. Glowinski, M. Imbert, and F.E. Bloom (eds): Molecular and Cellular Interactions Underlying Higher Brain Functions. Prog. Brain Res. *58:*313–319.

Rager, G., and U. Rager (1976) Generation and degeneration of retinal ganglion cells in the chicken. Exp. Brain Res. *25:*551–553.

Rakic, P., and K.P. Riley (1983a) Overproduction and elimination of retinal axons in the fetal rhesus monkey. Science *219:*1441–1444.

Rakic, P., and K.P. Riley (1983b) Regulation of axon number in primate optic nerve by prenatal binocular competition. Nature *305:*135–137.

Rakic, P. (1966) Mechanisms of ocular dominance segregation in the lateral geniculate nucleus: Competitive elimination hypothesis. Trends Neurosci. *9:*11–19.

Rapaport, D.H., and J. Stone (1982) The site of commencement of maturation in mammalian retina: Observations in the cat. Dev. Brain Res. *5:*273–279.

Rapaport, D.H., and J. Stone (1983) Time course of the morphological differentiation of cat retinal ganglion cells: Influences on cell size. J. Comp. Neurol. *221:*42–52.

Reh, T.A., and M. Constantine-Paton (1984) Retinal ganglion cell terminals change their projection sites during larval development of *Rana pipiens.* J. Comp. Neurol. *4:*442–457.

Reier, P.J., and A. Hughes (1972) Evidence for spontaneous axon degeneration during peripheral nerve maturation. Am. J. Anat. *135:*147–152.

Reier, P.J., and H. deF. Webster (1974) Regeneration and remyelination of *Xenopus* tadpole optic nerve fibres following transection or crush. J. Neurocytol. *3:*591–618.

Rhoades, R.W., L. Hsu, and G. Parfett (1979) An electron microscopic analysis of the optic nerve in the golden hamster. J. Comp. Neurol. *186:*491–504.

Robinson, A. (1896) On the formation and structure of the optic nerve, and its relation to the optic stalk. J. Anat., J. Physiol. (Lond.) *30:*319–333.

Roth, C.D., and K.C. Richardson (1969) Electron miscroscopical studies on axonal degeneration in the rat iris following ganglionectomy. Amer. J. Anat. *124:*341–360.

Rusoff, A.C., and W.R. Dubin (1977) Development of receptive field properties of retinal ganglion cells in kittens. J. Neurophysiol. *40:*1188–1198.

Scholes, J.H. (1981) Ribbon optic nerves and axonal growth patterns in the retinal projection to the tectum. In D.R. Garrod and J.D. Feldman (eds): Development in the Nervous System. Cambridge: Cambridge Univ. Press, pp. 181–214.

Schreyer, D.J., and E.G. Jones (1982) Growth and target finding by axons of the corticospinal tract in prenatal and postnatal rats. Neuroscience *8:*1837–1853.

Scott, T.M., and G. Lazar (1976) An investigation into the hypothesis of

shifting neuronal relationships during development. J. Anat. *121*:485–496.

Sefton, A.J., and K. Lam (1984) Quantitative and morphological studies on developing optic axons in normal and enucleated albino rats. Exp. Brain Res. *57*:107–117.

Sengelaub, D.R., and B.L. Finlay (1982) Cell death in the mammalian visual system during normal development: I. Retinal ganglion cells. J. Comp. Neurol. *204*:311–317.

Shatz, C.J., and M. Kliot (1982) Prenatal misrouting of the retinogeniculate pathway in the Siamese cat. Nature *300*:525–529.

Shatz, C.J. (1983) The prenatal development of the cat's retinogeniculate pathway. J. Neurosci. *3*:482–499.

Shatz, C.J., and P.A. Kirkwood (1984) Prenatal development of functional connections in the cat's retinogeniculate pathway. J. Neurosci. *4*:1378–1397.

Sherman, S.M., and P.D. Spear (1982) Organization of visual pathways in normal and visually deprived cats. Physiol. Rev. *62*:738–855.

Silver, J. (1984) Studies of the factors that govern directionality of axonal growth in the embryonic optic nerve and at the chiasm of mice. J. Comp. Neurol. *223*:238–251.

Silver, J., and R.M. Robb (1979) Studies on the development of the eyecup and optic nerve in normal mice and in mutants with congenital optic nerve aplasia. Dev. Biol. *68*:175–190.

Silver, J., and J. Sapiro (1981) Axonal guidance during development of the optic nerve: The role of pigmented epithelia and other extrinsic factors. J. Comp. Neurol. *202*:521–538.

Silver, J., and U. Rutishauser (1984) Guidance of optic axons *in vivo* by a preformed adhesive pathway on neuroepithelial endfeet. Dev. Biol. *106*:485–499.

Skoff, R.P. and V. Hamburger (1974) Fine structure of dendritic and axonal growth cones in embryonic chick spinal cord. J. Comp. Neurol. *153*:107–147.

Snedecor, G.W., and W.G. Cochran (1967) Statistical Methods (6th ed.). Ames, Iowa: The Iowa State University Press.

Sohol, G.S., and T.A. Weidman (1978) Development of the trochlear nerve: Loss of axons during normal ontogeny. Brain Res. *142*:455–465.

Speidel, C.C. (1933) Studies of living nerves. II. Activities of ameboid growth cones, sheath cells, and myelin segments, as revealed by prolonged observation of individual nerve fibers in frog tadpoles. Am. J. Anat. *52*:1–79.

Sretavan, D.W., and C.J. Shatz (1984) Prenatal development of individual retinogeniculate axons during the period of segregation. Nature *308*:845–848.

Sretavan, D.W., and C.J. Shatz (1986) Prenatal development of retinogeniculate axon arbors in the absence of binocular interactions. J. Neurosci., in press.

Stein, B.E., E. Labos, and L. Kruger (1973) Sequence of changes in properties of neurons of superior colliculus of the kitten during maturation. J. Neurophysiol. *36*:667–679.

Stein, B.S. (1975) The genital system. In E.J. Catcott (ed.): Feline Medicine and Surgery, 2nd ed., Santa Barbara, California: American Veterinary Pub. Inc., pp. 303–354.

Stone, J., D.H. Rapaport, R.W. Williams, and L.M. Chalupa (1982) Uniformity of cell distribution in the ganglion cell layer of prenatal cat retina: Implications for mechanisms of retinal development. Dev. Brain Res. *2*:231–242.

Straznicky, K., and R.M. Gaze (1971) The growth of the retina in *Xenopus laevis*: An autoradiographic study. J. Embryol. Exp. Morphol. *26*:67–79.

Suburo, A., N. Carri, and R. Adler (1979) The environment of axonal migration in the developing chick retina: A scanning electron microscopic (SEM) study. J. Comp. Neurol. *184*:519–536.

Sur, M., R.E. Weller, and S.M. Sherman (1984) Development of X- and Y-cell retinogeniculate terminations in kittens. Nature *310*:246–249.

Tennyson, V. (1970) The fine structure of the axon and growth cone of the dorsal root neuroblast of the rabbit embryo. J. Cell. Biol. *44*:62–79.

Tosney, K.W., and L.T. Landmesser (1985) Development of the major pathways for neurite outgrowth in the chick hindlimb. Dev. Biol. *109*:193–214.

Ulshafer, R.J., and A. Clavert (1979) Cell death and optic fiber penetration in the optic stalk of the chick. J. Comp. Neurol. *162*:67–76.

van Crevel, H., and W.J.C. Verhaart (1963) The rate of secondary degeneration in the central nervous system. II. Optic nerve of the cat. J. Anat. *97*:451–464.

Vaney, D.I., and A. Hughes (1976) The rabbit optic nerve: Fibre diameter spectrum, fibre count, and comparison with a retinal ganglion cell count. J. Comp. Neurol. *170*:241–252.

Vaughn, J.E., and T.J. Sims (1978) Axonal growth cones and developing axonal collaterals form synaptic junctions in embryonic mouse spinal cord. J. Neurocytol. *7*:337–363.

Vogel, M. (1978) Postnatal development of the cat's retina: A concept of maturation obtained by qualitative and quantitative examination. Albrecht v. Graefe's Arch. f. Ophthalmol. *208*:93–107.

von Szily, A. (1912) Über die enleitenden Vorgänge bei der ersten Entstehung der Nervenfasern im Nervus opticus. Albrecht von Graefe's Arch. f. Ophthalmol. *81*:67–86, plates V and VI.

Walsh, C., and E.H. Polley (1985) The topography of ganglion cell production in the cat's retina. J. Neurosci. *5*:741–750.

Walsh, C., E.H. Polley, T.L. Hickey, and R.W. Guillery (1983) Generation of cat retinal ganglion cells in relation to central pathways. Nature *302*:611–614.

Webster, H. deF. (1962) Transient, focal accumulation of axonal mitochondria during the early stages of Wallerian degeneration. J. Cell Biol. *12*:361–383.

Willard, M. (1983) Neurofilaments and axonal transport. In C.A. Marotta (ed): Neurofilaments. Minneapolis: University of Minnesota Press. pp. 86–116.

Williams, R.W., and L.M. Chalupa (1982) Prenatal development of retinocollicular projections in the cat: An anterograde tracer transport study. J. Neurosci. *2*:604–622.

Williams, R.W., and L.M. Chalupa (1983a) Development of the retinal pathway to the pretectum of the cat. Neuroscience *10*:1249–1267.

Williams, R.W., and L.M. Chalupa (1983b) An analysis of axon caliber within the optic nerve of the cat: Evidence of size groupings and regional organization. J. Neurosci. *3*:1554–1564.

Williams, R.W., M.J. Bastiani, and L.M. Chalupa (1983) Loss of axons in the cat optic nerve following fetal unilateral enucleation: An electron microscopic analysis. J. Neurosci. *3*:133–144.

Williams, R.W., and P.R. Rakic (1984) Form, ultrastructure, and selectivity of growth cones in the developing primate optic nerve: 3-dimensional reconstructions from serial electron micrographs. Soc. Neurosci. Abst. *10*:373.

Williams, R.W., J.W. Crabtree, L.M. Chalupa, P.D. Spear, and S.E. Kornguth (1985) Selectivity of antibody-mediated destruction of axons in the cat's optic nerve. Brain Res. *336*:57–66.

Williams, R.W., and P.R. Rakic (1985a) Dispersion of growing axons within the optic nerve of the embryonic monkey. Proc. Natl. Acad. Sci. U.S.A. *82*:3906–3910.

Williams, R.W., and P.R. Rakic (1985b) Deployment of ganglion cell growth cones in retina, optic nerve, and optic tract of rhesus monkeys. Invest. Ophthalmol. Vis. Sci. [Suppl.] *26*:286.

Wilson, M.A. (1971) Optic nerve fibre counts and retinal ganglion cell counts during development of *Xenopus laevis* (Daudin). Q. J. Exp. Physiol. *56*:83–91.

Winfield, D.A., R.W. Hiorns, and T.P.S. Powell (1980) A quantitative electron-microscopical study of the postnatal development of the lateral geniculate nucleus in normal kittens with eyelid suture. Proc. R. Soc. Lond. [Biol.] *210*:211–234.

Yamada, K.M., B.S. Spooner, and N.K. Wessells (1970) Axon growth: Roles of microfilaments and microtubules. Proc. Natl. Acad. Sci. U.S.A. *66*:1206–1212.

Yamada, K.M., B.S. Spooner, and N.K. Wessells (1971) Ultrastructure and function of growth cones and axons of cultured nerve cells. J. Cell Biol. *49*:614–635.